



Residential solid fuel combustion and its contribution to air pollution in Hungary: A comparative study

Boglárka S. Balogh^{a,b}, Zsófia Csáková^a, Zoltán Nyíri^a, Balázs Berlinger^{a,c}, Mihály Molnár^d, István Major^d, Virág Gergely^d, Tamás Szigeti^{a,*}

^a National Center for Public Health and Pharmacy, Albert Flórián út 2-6., 1097, Budapest, Hungary

^b Doctoral School of Environmental Sciences, Eötvös Loránd University, Pázmány Péter stry. 1/A., 1117, Budapest, Hungary

^c Department of Animal Hygiene, Herd Health and Mobile Clinic, University of Veterinary Medicine, István u. 2., 1078, Budapest, Hungary

^d International Radiocarbon AMS Competence and Training Center (INTERACT), HUN-REN Institute for Nuclear Research (ATOMKI), Bem tér 18/c, 4026, Debrecen, Hungary

HIGHLIGHTS

- Higher PM_{2.5} levels were observed during the heating season, notably in the rural area.
- Several biomass and waste burning markers were investigated.
- Considerable differences were obtained across the sampling sites.
- This study highlights the need for national and local efforts to cut emissions.

ARTICLE INFO

Keywords:

Air quality
Markers
Residential heating
Seasonal variation
Solid fuel combustion
Waste burning

ABSTRACT

Residential solid fuel combustion is a significant contributor to air pollution in Hungary, particularly in rural areas. This study aimed to assess air pollution attributable to residential solid combustion by monitoring the spatial and temporal variability of PM_{2.5} mass concentration and other specific air pollutants. Sampling campaigns were conducted at rural and urban sites with differing heating habits, comparing heating and non-heating periods in 2020.

Significant differences in air pollutant concentrations were observed between the two periods. At the rural site, the mean PM_{2.5} mass concentration was 1.7 times higher during the heating period compared to the urban site. Biomass burning markers (e.g. levoglucosan, potassium, organic carbon in PM_{2.5}) showed a significant association during the heating period. Additionally, the universal waste burning marker 1,3,5-triphenylbenzene was detected on 93% of the measurement days at the rural site during the heating period, indicating continuous waste burning. The results of ¹⁴C analysis and multiple diagnostic ratios further supported source identification. The annual target value for benzo(a)pyrene (1 ng/m³) was exceeded in 100% of samples collected at the rural site and 64% of samples at the urban site during the heating period. Detailed chemical analysis of PM_{2.5} accounted for an average of 85% of total mass.

These findings highlight the urgent need for robust national and local air quality strategies to mitigate emissions from residential heating and protect public health.

1. Introduction

Globally, over 2.3 billion people, about 40% of households, rely on solid fuels as their primary energy source (WHO, IEA, IRENA, UNSD, World Bank, 2022). Residential combustion of solid fuels contributes

substantially to air pollution, especially in areas lacking emission controls or using inefficient technologies (Klimont et al., 2017). Ambient air pollution is a major global health risk and has been linked to millions of premature deaths worldwide (Lelieveld et al., 2015). Evidence links emissions from wood, coal, and waste burning to serious health effects,

* Corresponding author. National Center for Public Health and Pharmacy, Hungary.

E-mail address: szigeti.tamas@nngyk.gov.hu (T. Szigeti).

<https://doi.org/10.1016/j.atmosenv.2025.121399>

Received 1 April 2025; Received in revised form 28 June 2025; Accepted 5 July 2025

Available online 6 July 2025

1352-2310/© 2025 The Authors. Published by Elsevier Ltd. This is an open access article under the CC BY license (<http://creativecommons.org/licenses/by/4.0/>).

including respiratory and cardiovascular morbidity and mortality (Balmes, 2019; Kim et al., 2015). A recent report estimates that 3.2 million people die prematurely each year from diseases attributable to household air pollution caused by the inappropriate use of solid fuels (WHO, 2021).

Residential solid fuel combustion has a major impact on air pollution, resulting in the emission of significant amounts of gas- and particle-phase pollutants, including inorganic gaseous compounds, particulate matter (PM), organic matter (OM), elemental carbon (EC), polycyclic aromatic hydrocarbons (PAHs), and various other organic compounds (Clark and Peel, 2013; Krugly et al., 2014; Simoneit, 2002). Globally, 20% of fine PM ($PM_{2.5}$) originates from residential fuel burning, which may contribute up to 32% of $PM_{2.5}$ emissions in Central and Eastern Europe (Karagulian et al., 2015).

A significant portion of Hungarian households still relies on solid fuels (e.g. wood, crop residues, coal, household waste) primarily for heating and, to a lesser extent, for cooking. Solid fuel burning is very common in Hungary: 62% of the dwellings use gas, 32% wood, 9% electricity, 1% coal, and 1% other fuels, with some dwellings relying on multiple fuel types (National Census, 2022).

The marker/tracer methods are based on the identification of substances that are directly related to solid fuel combustion emissions. These markers are essential for identifying such emissions as they are directly linked to specific types of burning (e.g. wood, waste) and can indicate the combustion efficiency. The most frequently investigated markers of solid fuel burning are monosaccharide anhydrides (MAs) (such as levoglucosan (LEV) and its isomers, mannosan (MAN) and galactosan (GAL)), organic carbon (OC), PAHs, potassium (K), and certain metals. In addition to water-soluble K as a well-known biomass burning (BB) tracer, LEV and its isomers are suitable markers for detecting wood burning, as they occur in large quantities and have longer stability compared to other organic tracers (Blumberger et al., 2019; Simoneit, 2002). 1,3,5-Triphenylbenzene (135-TPB) is a universal tracer compound for waste burning (Simoneit, 2015; Simoneit et al., 2005; Tomsej et al., 2018).

Source apportionment studies generally indicate that wood combustion accounts for 20–30 % of ambient $PM_{2.5}$ mass concentrations during the heating period; although, this estimate varies considerably by location (Braníš and Domasová, 2003; Caseiro et al., 2009; Gianelle et al., 2013). Several studies across Europe have investigated air pollution associated with wood burning, highlighting how its impact on ambient PM levels varies by season, source density, technology, meteorology, and topography (e.g. Cigánková et al., 2021; Maenhaut et al., 2016; Ricciardelli et al., 2017; Galindo et al., 2021; Janoszka and Czaplícka, 2022). Several studies focused on the characterization of $PM_{2.5}$ and PM_{10} in Hungary, providing quantitative information on some important source categories (e.g. Angyal et al., 2024; Blumberger et al., 2019; Major et al., 2021; Salma et al., 2017, 2020; Szigeti et al., 2015); however, source apportionment has rarely been carried out, especially for rural areas.

Despite legal prohibitions, household waste burning occurs in Hungary as a cost-saving measure for heating and waste disposal. Approximately 2–10% of the population has been reported to regularly burn their waste in stoves in Hungary, according to two independent surveys carried out a few years ago (Kantar Hoffmann, 2017; Századvég Foundation, 2018). In Hungarian households, solid fuel is often burned in inefficient, poorly ventilated heating appliances (e.g. conventional stoves, boilers), and incomplete combustion produces substances of public health concern. Only a limited number of scientific papers investigate waste burning with a particular emphasis on identifying suitable organic tracers in PM samples (Hoffer et al., 2021; Simoneit et al., 2005; Tomsej et al., 2018).

There has been a major effort to reduce the emission of air pollutants, especially $PM_{2.5}$ emissions, in the hot spot areas in Hungary, where there were difficulties complying with the limit values set by the European Commission. Three air quality zones have struggled to comply with the



Fig. 1. Location of the settlements selected for the monitoring campaign in Hungary.

European Union's Air Quality Directive 2008/50/EC, and as a result, the European Commission launched infringement proceedings against Hungary (European Commission, 2008). Due to frequent unfavorable meteorological conditions and higher PM emission rates, air quality is worse in winter than in summer in Hungarian settlements. Therefore, identifying the sources of PM is essential to provide decision-makers with appropriate recommendations for developing measures and regulations to reduce emissions.

The influence of residential solid fuel combustion on the air quality in Hungary is still poorly understood, so it is important to have a clear picture of its main characteristics. This study is unique in its comprehensive examination of the impact of residential solid fuel combustion on air quality in Hungary, particularly in rural settlements where such practices are common. Unlike previous research, which has often been limited in scope or geographical focus, our study provides an extensive analysis of a wide range of air pollutants, specifically those associated with $PM_{2.5}$. By focusing on both rural and urban sites with varying heating habits, we capture the spatial and temporal variability in air pollutant concentrations during heating and non-heating periods. This research provides new data from Hungary, where comprehensive aerosol measurements are relatively limited, and offers critical information that can inform policy decisions aimed at improving air quality both locally and in comparable international contexts. Through our investigation, we aim to provide a clear picture of the main characteristics of residential solid fuel combustion and its significant role in air pollution, supporting the development of more effective national and regional air quality management strategies.

2. Materials and methods

2.1. Description of the sampling sites

The monitoring campaign took place at two sites in North Hungary: one rural and one urban (Fig. 1). Nógrádmegyer, with a population of 1700 (GPS coordinates: 48° 04' 07" N, 19° 37' 26" E; 204 m above mean sea level), was selected as the rural site, where the use of solid fuel for heating and cooking purposes is significant. The municipality is located in a valley within the hilly region of northern Hungary, surrounded by gentle slopes. The selected urban site was Esztergom, with a population of 27,000 (GPS coordinates: 47° 47' 08" N, 18° 44' 25" E; 110 m above mean sea level), where the majority of households use either district heating or gas heating. Esztergom is located along the bank of the Danube River, featuring a varied topography with rolling hills, riverbanks, and elevated terrain. Both sampling sites were designated in the center of the settlements, in a residential area. The disturbing effect of traffic is negligible at the rural site, while a 2-lane busy road was close (at a distance of 70–80 m) to the sampling location at the urban site.

2.2. Sampling and instrumentation

Two, 14-day field campaigns, one during the heating period and another during the non-heating period, were implemented in 2020. The field campaigns were carried out from 27 January to 9 February and from 26 August to 9 September, respectively. These specific periods were selected to represent typical seasonal conditions while also aligning with the scheduling of a parallel human biomonitoring campaign (details not shown) and coordination with local organisations. Satellite-based fire detection data from NASA's FIRMS (MODIS, Terra/Aqua) were analysed for the sampling periods. According to the available data, no extensive agricultural burns or wildfires occurred within a 30 km radius of the settlements during these periods.

Meteorological parameters (temperature, relative humidity, wind direction, and wind velocity) were monitored at the fixed station of the National Air Quality Monitoring Network in Esztergom, located approximately 1 km from the selected sampling site, and at the sampling site in Nógrádmegyer using the mobile air quality monitoring station of the National Center for Public Health and Pharmacy. The values of meteorological variables were recorded with a time resolution of 1 h. Planetary boundary layer (PBL) height data were obtained from the ERA5 reanalysis dataset (Copernicus Climate Data Store, ECMWF) with hourly resolution.

The PM_{2.5} samples were collected for 24 h onto quartz fiber filters (Ø 150 mm, Whatman QM-A) by a Digitel DHA-80 high-volume aerosol sampler (Digitel Elektronik AG, Switzerland) equipped with a PM_{2.5} cut-off inlet in each site. The samplers were loaded with 14 filters, which were changed automatically every day at 6 p.m. The applied flow rate was 30 m³/h, thus about 720 m³ of air was pumped through a filter during the sampling time of 24 h. One field blank sample was also taken at each site per week. Before sampling, filters were wrapped in aluminium foil and pre-treated at 550°C in an electric oven for 8 h to eliminate any potential organic contaminants. Before and after sampling, the filters were conditioned for at least 48 h at 20 ± 1°C and 50 ± 5% relative humidity. The total PM_{2.5} mass was determined by weighing the sampling filters before and after sampling and the PM_{2.5} concentration was calculated by dividing the weighted mass on the filter by the sampling volume. Before analyses, filters were stored in glass Petri dishes sealed with parafilm at -20°C. Although the reference method described in EN 12341:2023 for the determination of PM_{2.5} mass concentration is based on low-volume samplers, the use of high-volume samplers in our study was primarily motivated by the need to collect sufficient PM_{2.5} mass for detailed chemical analysis. Previous studies (e. g. Viana et al., 2006) have reported differences between high- and low-volume sampling methods, particularly due to variations in face velocity. These differences can affect the measurement of certain PM components, such as OC. In fact, PM and OC concentrations obtained from low-volume samplers are often reported to be higher than those from high-volume samplers. This discrepancy is thought to result from a greater influence of positive artefacts in low-volume systems, as the adsorption of gaseous organic compounds tends to increase at lower face velocities.

Volatile organic compounds (VOCs) and carbonyls were collected by active sampling using a low-volume SKC Sidekick pump (SKC Ltd., United Kingdom) for 60 min every day from 6 p.m. to 7 p.m. This evening period was selected because residential activities, particularly heating, tend to increase after work hours, especially during the heating season when heating systems are typically activated. VOCs were collected onto a preconditioned TENAX-TA stainless steel tube (Markes International Ltd., UK) at a flow rate of 80 mL/min. Carbonyls were collected onto prepacked silica gel cartridge coated with 2,4-dinitrophenylhydrazine (DNPH) (dr. Weber Consulting Kft., Hungary) at a flow rate of 1 L/min. After sampling, the cartridges were capped and stored in a refrigerator at 4°C until analysis.

For the sampling of gas-phase PAHs, a polyurethane foam (PUF) sorbent was used. The sorbent was placed in a borosilicate glass tube,

which was connected to a low-volume SKC Sidekick pump operating at 2.5 L/min. The sampling time was 24 h and the sampling started at 6 p.m. every day. Before sampling, the PUF sorbent was purified by ultrasonic extraction in dichloromethane (Sigma-Aldrich, USA) and n-hexane (97%, LGC Standards, Germany). After sampling, the sample was stored in a hermetically sealed mason jar with a PTFE-coated screw cap at -20°C until sample preparation.

2.3. Assessment of the carbonaceous fractions

Circular punches with 1 cm diameter were analysed to measure the concentration of OC and EC by the thermal-optical method using the OCEC Lab Aerosol Analyzer (Sunset Laboratory Inc., USA) and the EUSAAR2 (European Supersites for Atmospheric Aerosol Research) protocol (Cavalli et al., 2010). The accuracy and repeatability of results were regularly controlled based on the determination of a sucrose solution containing 50 µg of carbon in 10 µL or by using reference filters.

¹⁴C measurement of the PM_{2.5} samples was performed on the Environ MICADAS AMS (developed by ETH-Zürich, Switzerland) installed at ATOMKI, Debrecen. The carbon mass of the aerosol samples was calculated from the pressure of the CO₂ obtained during the preparation. Besides the real samples, two ¹⁴C reference samples (IAEA-C9 and -C3) were also prepared under the same conditions as the aerosol samples and measured for ¹⁴C to check the quality of the preparation. Normalization of the ¹⁴C measurements was performed by measuring graphite targets made from NIST SRM 4990C oxalic acid II standards. The radiocarbon data were expressed as the fraction of modern carbon (f_M). It is defined as f_M = A_{SN}/A_{ON}, where the specific ¹⁴C activity of the sample (A_{SN}) and the standard (A_{ON}) is not age-corrected, but normalized with respect to isotope-fractionation (Reimer et al., 2004). The f_M was converted into the fraction of contemporary carbon (f_C) with a correction factor of 1.08 for the effect of combustion of older firewood (Heal et al., 2011); thus, the f_C was calculated as f_C = f_M/1.08. The f_C can range from 0 (pure fossil carbon) to 1 (pure modern carbon) and directly reflects the relative fossil and modern contribution to carbon, so the fraction of fossil carbon f_f = 1 - f_C (Major et al., 2015, 2021).

2.4. Determination of monosaccharide anhydride concentrations

Three stereoisomers of a MA of C₆H₁₀O₅, namely LEV (1,6-anhydro-β-D-glucopyranose), MAN (1,6-anhydro-β-D-mannopyranose), and GAL (1,6-anhydro-β-D-galactopyranose), were analysed by gas chromatography-mass spectrometry (GC-MS) after trimethylsilylation. A 0.8 cm diameter piece was cut out of the filter disc using a punch. The filter piece was spiked with 10 µL of internal standard (IS) (β-D-xylopyranose, TRC, Canada) and 2 mL of acetone was added. The sections were extracted in a 4 mL glass vial with 2 mL of absolute acetone in an ultrasonic bath (Reasonic Cleaner, KLN Ultraschall GmbH, Germany) for 15 min. After the decantation of the supernatant, the extraction step was repeated. The combined extract was filtered through a 0.22 µm pore size PTFE syringe filter. The sample extracts were evaporated to dryness under a stream of nitrogen (4.5, Messer Hungarogáz Kft., Hungary). At the end of the evaporation, 300 µL of acetone was pipetted into the vials and evaporated to dryness again. This ensures that the distillate has evaporated to dryness, leaving no moisture. The silylation reaction was performed by adding 50 µL of pyridine as a solvent and 50 µL of a silylation mixture containing 1% (V/V) trimethylchlorosilane (TMCS) in N-Methyl-N-(trimethylsilyl)-trifluoroacetamide (MSTFA), all reagents sourced from Sigma-Aldrich (St. Louis, USA). The mixture was thermostated at 80°C for 60 min. The standards of MAs were purchased from Toronto Research Chemicals (Canada).

The GC-MS analysis was carried out using an Agilent 6890 Plus GC and 5973 quadrupole MS with 7683 autosampler (Agilent Technologies, USA). An Rxi-5Sil MS capillary column (l = 30 m, ID = 0.25 mm, dF = 0.25 µm) (Restek, USA) was used for the analysis. The GC conditions were as follows: the column starting temperature was 80°C, held for 0.3

min, which was then raised to 175°C with a rate of 40 °C/min, then to 205°C at 8 °C/min and then heated up to 300°C with a rate of 40 °C/min and finally held at this temperature for 2 min. The inlet temperature was maintained at 280°C. The GC was operated with a 20:1 split ratio and with a 1 mL/min column flow rate using helium (in purity of 5.0) as carrier gas. A sample volume of 1 µL was injected onto the column. Quantification is performed using IS matrix calibration, and the qualitative information is provided by retention times and peak area ratios of selected ions. The quantification was carried out in the selected ion monitoring mode by quantifier ions with mass-to-charge ratios (m/z) of 204 for LEV and m/z of 217 for MAN and GAL.

2.5. Investigation of polycyclic aromatic hydrocarbons

Approximately 1/8 of each loaded/blank filter was cut out with a ceramic lance and spiked with 50 µL of a deuterated standard solution (naphthalene- d_8 , acenaphthene- d_{10} , phenanthrene- d_{10} , chrysene- d_{12} , perylene- d_{12}). The ultrasonic liquid-solid extraction of the sample and the PAH analysis was conducted by following the procedure described in EN 15549:2008. Each filter piece was extracted in a 40 mL glass vial with 15 mL of n-hexane (97%, LGC Standards, Germany) in an ultrasonic bath for 10 min. After decantation of the supernatant, the extraction step was repeated. Then 5 mL of Milli-Q water was added to the collected extract, followed by intensive shaking by hand for 1 min and centrifugation at 2000 rpm for 5 min. After the extraction was completed, approx. 2–3 g of anhydrous Na_2SO_4 (Sigma-Aldrich, USA) was added to the supernatant. Finally, the contents were filtered by a filter paper (Schleicher & Schuell GmbH, Germany), concentrated to 1 mL by rotary evaporator and under a gentle nitrogen stream (4.5, Messer Hungarogáz Kft., Hungary), and then 20 µL of 2-fluorobiphenyl solution was added. The final extracts were stored in a freezer (-20°C) in sealed GC vials. To determine the concentration of gas-phase PAHs, the sorbents were stored in a freezer at -20°C until they were extracted. Extraction was performed as soon as possible to ensure minimal loss of volatile PAH species. The procedure applied for PAHs pre-treatment was Soxhlet extraction. Briefly, the PUF samples were put in a Soxhlet apparatus, spiked with a deuterated standard solution and extracted in n-hexane (97%, LGC Standards, Germany) for 24 h. Then the sample preparation steps described for the solid-phase PAH determination were followed as mentioned above. The detailed pre-treatment procedure can be found elsewhere (Mai et al., 2003). The quantitative determination of 20 particulate- and gas-phase PAHs was carried out by a GC (Agilent 6890 Plus) coupled with a mass selective quadrupole detector (Agilent 5973 MS) with an electron impact (EI) ionization source and Agilent 7683 autosampler. A DB-5MS UI capillary column ($l = 30$ m, $ID = 0.25$ mm, $dF = 0.25$ µm) was used for PAH separation. The chromatographic conditions were as follows: injector temperature: 300°C, detector temperature: 230°C and maximum oven temperature: 300°C. A sample volume of 1 µL was injected with pulsed splitless mode and with a column flow rate of 1.1 mL/min using helium (in purity of 6.0) as carrier gas. Nineteen US EPA analytical grade PAHs (EPA 8310 Polynuclear Aromatic Hydrocarbons Mix), the deuterated standards and 135-TPB were purchased from Sigma-Aldrich. 1,2,4-triphenylbenzene (124-TPB) was purchased from TCI Europe (Belgium).

2.6. Assessment of micro and trace elements concentrations

For trace element analysis two approx. 1/6 pieces were cut from the quartz fiber filters by a ceramic lance and their weight was measured. Then the samples underwent a microwave-assisted *aqua regia* extraction by using a Microwave LabStation (EM-45/A; Milestone Srl., Italy). The filter pieces were treated with 8 mL of *aqua regia* (6 mL of 34–37% hydrochloric acid and 2 mL of 67–69% nitric acid solution) for 30 min. Following the digestion, the solution was filtered through a 0.45-µm pore size PES syringe filter (VWR International Kft., Hungary) and diluted with high purity water to 25 mL. Before analysis, an IS solution

containing Sc, Ge, Y, Ir, Bi and Th was added to the 10 mL solution. The samples were stored in a freezer at -20°C until analysis.

In contrast, the determination of the four microelements (Na, K, Ca, Mg) was performed using a simple water extraction method. One-sixth of each filter was placed into a 50 mL polyethylene centrifuge tube, to which 50 mL of deionized water was added. The samples were then subjected to a 150-min sonication-assisted water extraction at room temperature by using an ultrasonic bath. After sonication, the solutions were filtered by applying a 0.22-µm pore size PES syringe filter. The extracted solution was then divided for further analyses as follows: 10 mL for the determination of water-soluble microelements, 15 mL for the determination of water-soluble anions, 5 mL for ammonium determination. Before analysis, 100 µL nitric acid and ISs were added into 10 mL filtered solution.

The concentration of 4 micro (Na, K, Ca, Mg) and 20 trace elements (Al, As, B, Ba, Cd, Co, Cr, Cu, Fe, Mn, Mo, Ni, Pb, Se, Sn, Sr, Ti, V, Zn) were determined by an iCAP RQ (Thermo Fisher Scientific GmbH, Germany) inductively coupled plasma mass spectrometer (ICP-MS). The analytical results for the exposed filters were corrected for the blank values.

2.7. Determination of water-soluble anions and ammonium ion

After sonication-assisted water extraction and filtration, 15 mL from each sample was diluted five times and subjected to ion chromatographic analysis. All measurements were carried out on a Thermo Scientific Dionex ICS-5000 (Thermo Fisher Scientific Inc., USA) instrument. Anions (SO_4^{2-} , NO_3^- , Cl^-) were separated on a Dionex IonPac™ AS11-HC ($l = 250$ mm, $ID = 2$ mm) analytical column (Thermo Fisher Scientific Inc., USA) by applying isocratic elution with 10 mM KOH at a flow rate of 0.38 mL/min. The column temperature was 25°C. A 10 µL aliquot of each sample/standard was loaded to the eluent stream. The ions were detected by the suppressed conductivity of the eluent.

The determination of NH_4^+ concentration was performed using a spectrophotometric method. A 5 mL aliquot of the filtered and extracted sample was diluted to 25 mL, followed by the addition of 2.5 mL color-forming reagent and 2.5 mL of an oxidizing reagent. Ammonium reacted with salicylate and hypochlorite in the presence of sodium nitro-ferricyanide (III) dihydrate. The absorbance of the resulting blue compound was measured at 655 nm on a Shimadzu UV-1800 spectrophotometer (Shimadzu Corporation, Japan).

2.8. Investigation of volatile organic compounds and carbonyls

Selected VOCs (benzene, toluene, ethylbenzene, m-, p-, and o-xylene, styrene, cyclopentanone, allylbenzene, and decane) were quantified using a thermal desorption (TD) unit (TD-100, Markes International Ltd., UK) coupled with a GC-MS/MS system consisting of an Agilent 7800 gas chromatograph (Agilent Technologies Inc., USA) and a 7000C triple quadrupole mass spectrometer. The GC was equipped with an EI ion source, and the collision gases used were 6.0-grade helium and 6.0-grade nitrogen. The carrier gas was 6.0-grade helium.

The samples were prepared by adding 1 µL of fluorobenzene methanolic working solution under a gentle nitrogen stream (~100 mL/min) for 2 min. DiffLok caps were placed on the TD tubes before inserting them into the TD automated sample introduction unit. Pre-desorption included a single dry purge at a flow rate of 20 mL/min for 1 min to remove residual moisture. Desorption was performed at 300°C for 10 min while the secondary trap temperature was maintained at -10°C using a Markes Unity Series Cold Trap packed with TENAX. After primary trap desorption, the secondary trap was desorbed at 280°C for 3 min to transfer the analytes to the GC-MS system.

The analytes were passed through a heated transfer line and refocused onto an HP-PONA capillary column (Agilent Technologies Inc., USA) with the following specifications: $l = 50$ m, $ID = 0.2$ mm, $dF = 0.5$ µm. The oven temperature was programmed to start at 35°C, held for 3

Table 1
Descriptive statistics of the air pollutants in the two settlements in the heating period.

	Rural site (Nógrádmegyer)						Urban site (Esztergom)					
	Min.	P25	Median	Mean	P75	Max.	Min.	P25	Median	Mean	P75	Max.
PM_{2.5} mass concentration (µg/m³)	8.86	16.6	24.5	27.3	31.6	63.4	3.09	10.9	15.3	16.0	21.1	30.9
Carbonaceous fractions (µg/m³)												
OC	2.88	5.39	7.48	9.51	11.8	25.9	1.59	3.03	4.99	5.17	6.74	9.70
EC	0.58	1.17	1.99	2.27	3.01	4.85	0.36	0.84	1.26	1.42	2.16	2.53
TC	3.47	6.73	9.38	11.8	14.7	30.7	1.95	3.87	6.26	6.59	9.02	12.1
f _c value of TC	0.82	0.85	0.88	0.88	0.90	0.998	0.75	0.82	0.87	0.86	0.91	0.94
f _f value of TC	0.002	0.10	0.12	0.12	0.15	0.18	0.06	0.09	0.13	0.14	0.18	0.25
Contemporary carbon	2.85	5.97	8.34	10.5	13.0	29.1	1.47	3.82	5.35	5.66	7.27	10.8
Fossil carbon	0.02	0.62	1.23	1.34	1.79	3.48	0.48	0.60	0.65	0.75	0.89	1.20
Monosaccharide anhydrides (ng/m³)												
Levoglucosan	235	634	942	1117	1349	3262	147	411	624	750	1156	1417
Mannosan	24.3	44.4	63.4	75.9	87.4	223	18.2	38.0	58.6	69.2	103	143
Galactosan	10.4	20.6	31.6	39.0	49.0	111	9.54	20.5	26.6	30.7	45.3	55.0
Water-soluble ions and micro elements (µg/m³)												
SO ₄ ²⁻	0.52	1.041	1.37	1.42	1.76	2.38	0.47	0.79	1.06	1.14	1.57	1.91
NO ₃ ⁻	0.38	1.27	1.63	1.80	2.04	3.73	0.45	0.99	1.90	2.01	2.77	4.83
Cl ⁻	<LOQ	<LOQ	<LOQ	0.13	0.13	0.40	<LOQ	<LOQ	0.15	0.13	0.18	0.24
NH ₄ ⁺	0.066	0.20	0.39	0.46	0.63	1.29	0.070	0.19	0.50	0.57	0.91	1.17
Na	0.34	0.36	0.39	0.41	0.42	0.73	0.33	0.37	0.40	0.41	0.42	0.54
K	0.19	0.43	0.66	0.81	0.97	2.53	0.07	0.16	0.31	0.32	0.40	0.64
Ca	0.068	0.082	0.12	0.12	0.15	0.20	0.11	0.12	0.14	0.18	0.24	0.35
Mg	0.029	0.033	0.042	0.041	0.045	0.059	0.034	0.036	0.043	0.044	0.051	0.062
Aqua regia extractable part of trace elements (ng/m³)												
Ti	0.20	0.73	2.89	3.02	4.76	7.41	0.90	1.47	3.07	2.78	3.94	5.04
V	0.19	1.31	1.53	1.63	2.06	2.54	0.58	0.91	1.03	0.98	1.09	1.22
Cr	4.75	5.32	5.77	6.54	7.94	9.40	2.49	3.69	4.18	4.07	4.49	4.93
Mn	0.80	1.39	1.81	2.29	3.41	4.26	0.62	1.74	2.62	5.39	5.29	28.7
Fe	17.0	29.6	44.5	63.5	94.3	141	14.8	33.8	42.1	52.2	58.4	137
Co	<LOQ	<LOQ	<LOQ	<LOQ	0.04	0.05	<LOQ	<LOQ	0.04	0.04	0.05	0.07
Ni	<LOD	<LOQ	0.45	0.71	0.88	2.82	<LOD	<LOQ	<LOQ	0.34	0.40	0.44
Cu	0.55	0.85	1.23	1.26	1.49	3.36	0.68	0.83	1.16	1.48	1.85	3.40
Zn	24.3	27.3	35.4	38.9	45.1	62.9	<LOD	13.2	17.3	16.7	18.3	25.1
As	<LOD	<LOQ	0.40	0.47	0.65	1.27	<LOQ	<LOQ	0.33	0.35	0.53	1.23
Sr	<LOD	<LOQ	<LOQ	1.54	2.08	3.97	<LOD	<LOQ	1.18	1.13	1.32	1.79
Cd	<LOD	1.84	3.18	9.91	8.11	71.3	<LOD	2.05	3.47	5.83	7.72	23.9
Sn	<LOQ	<LOQ	0.34	0.34	0.47	0.62	<LOQ	0.30	0.42	0.45	0.60	0.83
Sb	0.12	0.14	0.40	0.93	1.08	3.11	0.03	0.08	0.10	0.14	0.19	0.42
Ba	1.25	1.85	2.11	3.06	4.17	6.74	1.09	2.65	3.55	3.36	1.09	2.65
Pb	2.86	4.63	6.78	7.57	10.9	15.4	0.56	2.08	4.07	6.68	8.27	34.9
Particle phase PAHs (ng/m³)												
NAP, 2-MNAP, 1-MNAP, ACY, ACE, FLU, ANT	<LOD	<LOD	<LOD	<LOD	<LOD	<LOD	<LOD	<LOD	<LOD	<LOD	<LOD	<LOD
FLT	0.40	0.87	1.21	2.40	3.54	8.21	0.34	0.67	1.09	1.40	1.66	4.29
PYR	0.42	1.01	1.35	2.72	4.51	8.76	0.36	0.73	1.19	1.40	1.71	3.92
BaA	1.06	2.06	4.51	5.72	7.81	17.2	0.44	0.65	1.40	1.72	2.53	3.91
CHY	2.18	3.82	6.29	9.08	11.2	27.4	0.74	1.23	2.32	3.02	4.44	6.81
124-TPB	<LOD	<LOD	<LOQ	<LOQ	0.12	0.25	<LOD	<LOD	<LOD	<LOD	<LOD	<LOQ
135-TPB	<LOQ	0.21	0.32	0.43	0.60	0.91	<LOQ	0.13	0.15	0.77	0.29	5.51
BbF	2.87	4.21	7.31	7.78	8.45	20.9	0.98	2.52	3.16	3.51	4.79	6.90
BeP	1.04	1.55	2.38	2.68	2.81	7.81	0.36	0.85	1.08	1.18	1.61	2.23
BaP	1.06	2.02	3.00	3.81	3.74	13.2	0.42	0.76	1.36	1.50	2.07	3.30
DahA	0.29	0.40	0.55	0.65	0.67	1.85	<LOQ	0.24	0.32	0.31	0.41	0.57
IND	1.26	1.75	2.61	2.96	2.81	8.94	0.43	0.96	1.32	1.38	1.90	2.67
BghiP	1.09	1.51	1.97	2.34	2.10	7.19	0.36	0.77	1.03	1.08	1.45	2.09
Gas phase PAHs (ng/m³)												
NAP	2.87	5.36	8.72	9.01	12.8	18.2	2.67	5.59	7.06	8.37	10.4	17.2
2-MNAP	1.89	3.38	3.90	4.16	4.60	7.45	1.31	2.63	3.19	3.50	4.12	6.40
1-MNAP	1.14	2.23	2.53	2.76	3.13	5.25	0.81	1.64	1.99	2.21	2.66	4.24
ACY	<LOQ	1.52	2.79	2.77	4.04	6.04	<LOQ	0.57	1.06	1.55	2.59	4.67
ACE	0.29	0.50	0.58	0.60	0.78	0.87	<LOQ	0.34	0.44	0.45	0.59	0.88
FLU	0.80	1.28	1.82	1.88	2.62	2.95	0.31	0.79	1.01	1.20	1.66	2.52
ANT	<LOQ	0.41	0.57	0.65	0.94	1.30	<LOQ	<LOQ	<LOQ	0.17	0.34	0.52
FLT	0.51	1.08	1.46	2.15	2.36	5.95	<LOQ	0.63	0.91	0.93	1.03	1.96
PYR	0.32	0.71	0.92	1.43	1.78	4.03	<LOQ	0.44	0.60	0.62	0.70	1.33
BaA, 135-TPB	<LOQ	<LOQ	<LOQ	<LOQ	<LOQ	<LOQ	<LOQ	<LOQ	<LOQ	<LOQ	<LOQ	<LOQ
CHY	<LOD	<LOQ	<LOQ	<LOQ	<LOQ	<LOQ	<LOD	<LOQ	<LOQ	<LOQ	<LOQ	<LOQ
124-TPB, BbF, BkF, BeP, BaP, DahA, IND, BghiP	<LOD	<LOD	<LOD	<LOD	<LOD	<LOD	<LOD	<LOD	<LOD	<LOD	<LOD	<LOD
Volatile organic compounds (µg/m³)												
Benzene	0.62	1.98	4.81	5.86	10.0	13.0	0.36	1.31	2.08	2.03	2.48	4.35
Toluene	<LOQ	0.83	1.93	2.15	3.47	4.88	<LOQ	0.81	1.20	1.24	1.58	2.62
Ethylbenzene	<LOQ	<LOQ	<LOQ	<LOQ	<LOQ	0.60	<LOQ	<LOQ	<LOQ	<LOQ	<LOQ	1.63
m + p + o-Xylene	<LOQ	1.25	1.48	1.71	2.26	3.37	<LOD	<LOQ	<LOQ	1.44	<LOQ	9.14
Styrene	<LOQ	<LOQ	<LOQ	<LOQ	<LOQ	0.99	<LOQ	<LOQ	<LOQ	<LOQ	<LOQ	1.04
Ciklopentanon	<LOQ	<LOQ	<LOQ	<LOQ	<LOQ	<LOQ	<LOQ	<LOQ	<LOQ	<LOQ	<LOQ	<LOQ

(continued on next page)

Table 1 (continued)

	Rural site (Nógrádmegyer)						Urban site (Esztergom)					
	Min.	P25	Median	Mean	P75	Max.	Min.	P25	Median	Mean	P75	Max.
Allilbenzene	<LOQ	<LOQ	<LOQ	<LOQ	<LOQ	<LOQ	<LOQ	<LOQ	<LOQ	<LOQ	<LOQ	<LOQ
Decane	<LOD	<LOQ	<LOQ	<LOQ	<LOQ	<LOQ	<LOQ	<LOQ	<LOQ	0.52	<LOQ	1.05
Carbonyls ($\mu\text{g}/\text{m}^3$)												
Formaldehyde	<LOQ	1.61	3.79	4.64	7.13	12.4	<LOQ	<LOQ	1.63	2.47	3.87	6.01
Acetaldehyde	<LOQ	1.04	2.73	3.04	4.55	7.11	<LOQ	<LOQ	2.44	3.64	4.63	13.9
Hexaldehyde	<LOQ	<LOQ	<LOQ	0.98	<LOQ	1.84	<LOQ	<LOQ	<LOQ	1.18	1.58	2.08
Benzaldehyde	<LOQ	<LOQ	<LOQ	<LOQ	<LOQ	1.36	<LOQ	<LOQ	<LOQ	<LOQ	<LOQ	<LOQ

min, then increased at a rate of 10 °C/min to 220°C, and held at this temperature for 2 min. The carrier gas flow rate was maintained at 2 mL/min.

The analysis of aldehydes during active sampling was performed using a liquid chromatography method (HPLC-DAD) in accordance with the ISO 16000-3:2011 standard. Regarding the selected carbonyls (formaldehyde, acetaldehyde, hexaldehyde, benzaldehyde; standards purchased from Sigma Aldrich, USA), the cartridges were extracted with 3 mL of acetonitrile in an ultrasonic bath for 30 min, then the extracts were filtered through a 0.22 μm pore size PTFE syringe filter. The extracts were analysed by high-performance liquid chromatography. The applied liquid chromatographic system consisted of an Agilent Series 1260 system (Agilent Technologies, Inc., Santa Clara, CA), composed of a G1321B binary pump, a G4225A degassing device, a G1329B autosampler, and an Agilent 1290 DAD G4212A diode array detector set at 360 nm. The chromatographic separation was performed on an Agilent Rapid Resolution HD Zorbax Eclipse Plus C18 column (100 mm \times 2.1 mm \times 1.8 μm) and 2 μL of analytes was injected onto the column. The mobile phase consisted of a gradient of acetonitrile and aqueous phosphoric acid solution (pH = 2.6), and the analyses were conducted with a constant flow rate of 0.4 mL/min (injection volume of 2 μL) and at a constant column temperature of 40°C.

2.9. Statistical analysis

Values below the LOD were substituted by one-half of the LOD for the calculations. In the case of values between the LOD and LOQ, raw values given by the laboratory were kept for the statistical analyses. Descriptive analysis (minimum, 25th percentile, median, mean, 75th percentile, maximum) for all the analysed compounds was performed. The Shapiro-Wilk test was used to examine the normality of data. As most variables did not follow a normal distribution, non-parametric methods were applied throughout the analysis. The Kruskal-Wallis test was used to evaluate the difference in PM characteristics at the two sampling locations and periods. A statistically significant level was considered when p-value was below 0.05. All analyses were performed using SPSS ver. 22.0 (IBM Corp., Armonk, NY, USA).

3. Results

The results of the monitoring campaigns for the investigated air pollutants are listed in Table 1 and Table A.1 for the heating and non-heating periods, respectively. The minimum, maximum, mean and median concentration values and the 25th and 75th percentiles are shown in the tables.

3.1. Meteorology

The meteorological parameters are listed in Table A.2 and A.3. The meteorological data recorded during the heating period aligned with typical monthly mean values; however, January was slightly milder and windier than the average for this time of year. There were no significant differences in the temperature and relative humidity values between the two locations. During the heating period, the daily mean temperature

values ranged from -1.6 to 11.1°C, while the relative humidity values ranged from 53.9 to 99.4%. In the non-heating period, the daily mean temperature values ranged from 14.4 to 27.1°C, and relative humidity values ranged from 51.6 to 84.7%. Significant precipitation (5–15 mm) occurred between the 5th and 7th measurement days in both settlements.

3.2. Air pollutants

3.2.1. $\text{PM}_{2.5}$

The highest $\text{PM}_{2.5}$ mass concentrations were observed in Nógrádmegyer during the heating period, with daily mean values ranging from 8.86 to 63.4 $\mu\text{g}/\text{m}^3$ and a median value of 24.5 $\mu\text{g}/\text{m}^3$. The median daily mean $\text{PM}_{2.5}$ mass concentration in Esztergom was 0.62 times lower than in Nógrádmegyer during the heating period. Significant seasonal differences in $\text{PM}_{2.5}$ mass concentrations were observed. In Nógrádmegyer and Esztergom, the median daily mean $\text{PM}_{2.5}$ mass concentrations were 2.2 and 1.8 times higher during the heating period compared to the non-heating period, respectively. The WHO's 24-h $\text{PM}_{2.5}$ guideline value of 15 $\mu\text{g}/\text{m}^3$ was exceeded in 79 and 50% of the samples collected during the heating period in Nógrádmegyer and Esztergom, respectively. During the non-heating period, the guideline value was exceeded only in Nógrádmegyer, with 22% of the values higher than 15 $\mu\text{g}/\text{m}^3$.

3.2.2. Carbonaceous fractions

Considerable spatial and temporal changes were observed in the carbonaceous fractions. OC, EC, and TC all showed temporal variations, with peak concentrations during the heating period. Overall, OC concentrations were 1.7 times higher in the rural site than in the urban site across the study period. In the heating period, OC concentrations ranged from 2.9 to 25.9 $\mu\text{g}/\text{m}^3$ in Nógrádmegyer (mean: 9.5 $\mu\text{g}/\text{m}^3$) and from 1.6 to 9.7 $\mu\text{g}/\text{m}^3$ in Esztergom (mean: 5.2 $\mu\text{g}/\text{m}^3$). The mean OC concentrations during the heating period were 3.2 and 2.1 times higher at the rural and urban sites compared to the values obtained for the non-heating period, respectively, similar to the ratio of 2.9 observed for Budapest in a previous study (Szigeti et al., 2015). The mean EC concentrations were 2.2 and 1.8 times higher during the heating period compared to the non-heating period in Nógrádmegyer and Esztergom, respectively, following a similar trend to OC. Overall, the observed OC, EC, and TC concentrations align with previous results from similar locations in Hungary (Salma et al., 2004; Szigeti et al., 2015; Major et al., 2021) and other European settlements (Bressi et al., 2013; Putaud et al., 2004), with higher mean OC and EC levels at rural sites during heating periods as expected.

To differentiate modern or contemporary and fossil sources, f_c and f_f values were determined daily during the sampling period. Mean f_c values were 0.76 in Nógrádmegyer and 0.74 in Esztergom, indicating that modern sources were consistently dominant at both sites. During the heating period, biogenic fractions were observed with mean values of 0.88 in Nógrádmegyer and 0.86 in Esztergom, suggesting minimal fossil contributions at this time. Conversely, fossil carbon peaks, coinciding with contemporary carbon minima, occurred in the non-heating period with mean values of 0.37 in Nógrádmegyer and 0.36 in

Esztergom.

Mean contemporary carbon concentrations were 10.5 and 2.39 $\mu\text{g}/\text{m}^3$ in Nógrádmegyer and 5.66 and 2.35 $\mu\text{g}/\text{m}^3$ in Esztergom for the heating and non-heating periods, respectively. Contemporary carbon levels during the heating period were 4.4 and 2.4 times higher than summer levels in Nógrádmegyer and Esztergom, respectively. Fossil carbon concentrations followed a different temporal pattern, with mean values of 1.34 and 1.41 $\mu\text{g}/\text{m}^3$ in Nógrádmegyer and 0.75 and 1.04 $\mu\text{g}/\text{m}^3$ in Esztergom for the heating and non-heating periods, respectively. Higher fossil carbon concentrations were noted in the non-heating period.

3.2.3. Monosaccharide anhydrides (MAs)

LEV was the most abundant MA, followed by MAN and GAL. LEV concentrations were significantly higher than the combined levels of MAN and GAL in both periods, with concentrations approximately 1.5 times higher at the rural site than at the urban site. During the heating period, the mean concentrations were 1117 ng/m^3 for LEV, 75.9 ng/m^3 for MAN, and 39.0 ng/m^3 for GAL in Nógrádmegyer. A similar trend was observed in Esztergom, where mean concentrations during the heating period were slightly lower: 750 ng/m^3 for LEV, 69.2 ng/m^3 for MAN, and 30.7 ng/m^3 for GAL. The MA concentrations in the heating period showed considerable variations, with LEV ranging from 234 to 3262 ng/m^3 , MAN from 18.2 to 223 ng/m^3 , and GAL from 9.5 to 111 ng/m^3 . In contrast, the MA concentrations in the non-heating period were significantly lower, with LEV concentrations about 30 times lower than in the heating period, ranging from 8.5 to 92.2 ng/m^3 .

3.2.4. Polycyclic aromatic hydrocarbons

Table 1 presents the individual concentrations of PAHs in both the gas and particulate phases. Although all 20 analysed PAH compounds were detected at both sites, it is important to note that low-molecular-weight (LMW) PAHs were not detectable in the particulate phase, while high-molecular-weight (HMW) PAHs were not detectable in the gas phase due to significant differences in their volatility. Consistent with the trends observed for $\text{PM}_{2.5}$ mass and MAs concentrations, PAH levels were higher in Nógrádmegyer than in Esztergom during both the heating and non-heating periods. On average, PAHs contributed approximately 0.20 and 0.10% of the $\text{PM}_{2.5}$ mass concentration in Nógrádmegyer and Esztergom, respectively. Throughout the study, total PAH concentrations in the particle phase were significantly higher than those in the gas phase. In Nógrádmegyer, summed (gas + particle phase) PAH concentrations ranged from 26.8 to 188 ng/m^3 , with a mean value of 76.1 ng/m^3 . In Esztergom, summed PAH concentrations ranged from 16.0 to 93.4 ng/m^3 , with a mean value of 45.5 ng/m^3 .

LMW PAHs with 2–3 aromatic rings were the most abundant, contributing 40 and 56% of total PAHs at the rural and urban sites, respectively. Middle-molecular-weight (MMW) PAHs (4-ring) accounted for 33% at the rural site and 25% at the urban site, while HMW PAHs with 5–6 rings made up a smaller proportion, contributing 27 and 19% at the rural and urban sites, respectively. The most abundant particle-phase PAHs was CHY (<LOD–27.4 ng/m^3), followed by BbkF (2.87–20.9 ng/m^3) and BaA (1.06–17.2 ng/m^3). In the gas phase, NAP (2.87–18.2 ng/m^3), 2-MNAPH (1.89–7.45 ng/m^3), 1-MNAPH (1.14–5.25 ng/m^3), and ACE (<LOQ–6.04 ng/m^3) were the most abundant PAHs. Gas-phase concentrations were approximately an order of magnitude lower than those in the particle phase for most compounds.

The International Agency for Research on Cancer (IARC) lists BaP as a Group 1 carcinogen, making it one of the most monitored PAHs in ambient air (IARC, 2016). DahA is classified as probably carcinogenic to humans (Group 2A), while some PAHs, including NAP, BaA, BbF, BkF, CHY, and IND, are considered Group 2B, possibly carcinogenic to humans (IARC, 2016). On average, PAHs classified as Group 1, 2A, and 2B (NAP, BaA, BbF, BkF, CHY, BaP, IND, and DahA) contributed 52 and 50% to the total measured PAH mass at rural and urban sites,

respectively, during the heating period. These findings align with previous studies of $\text{PM}_{2.5}$ -bound PAH levels at monitoring sites across Europe, including observations in Hungary (Gelencsér et al., 2007; Nagy and Szabó, 2019) and other European cities (Szidat et al., 2009).

3.2.5. Major water-soluble ions and micro elements

Considerable seasonal differences were observed in the concentrations of NH_4^+ , Na, K, Ca, NO_3^- , and Cl^- , with the highest levels occurring during the heating period. In contrast, SO_4^{2-} remained relatively constant throughout the year, with a slight decrease observed in summer. Although photochemical oxidation of SO_2 is typically more active in summer, the lower SO_4^{2-} concentrations are more likely due to reduced SO_2 emissions (e.g. absence of residential heating) and enhanced atmospheric dispersion, such as increased mixing layer height. It is well known that significant evaporation loss of ammonium nitrate occurs when measuring $\text{PM}_{2.5}$ concentrations during warm months, resulting in its particle phase concentration being significantly higher in winter compared to summer (Lim et al., 2021). Differences were also observed in the dominant anions and cations between the two sites. At the urban site, NO_3^- concentrations were similar to or greater than those of SO_4^{2-} , while SO_4^{2-} concentrations were higher than NO_3^- at the rural site. The K concentrations ranged from 0.02 to 2.53 $\mu\text{g}/\text{m}^3$ in Nógrádmegyer and from 0.03 to 0.64 $\mu\text{g}/\text{m}^3$ in Esztergom. During the heating period, the mean K concentration was 0.81 $\mu\text{g}/\text{m}^3$ at the rural site and 0.32 $\mu\text{g}/\text{m}^3$ at the urban site. In the rural site, K concentrations were higher than those of NH_4^+ and Na, whereas at the urban site, they were lower. The concentrations of NO_3^- and SO_4^{2-} were higher than those of other ions, accounting for 60.5–66.7% of the total mass of water-soluble ions in each period, while Cl^- contributed less than 2% of the total mass of ionic species.

3.2.6. Trace elements

Among the 16 elements analysed, Fe - a typical crustal element - was the most abundant in $\text{PM}_{2.5}$ followed by the non-crustal trace metals such as Zn, Cd, Pb, and Cr. Of the elements investigated, only Fe exceeded the concentration level of 100 ng/m^3 , while Co was present at the lowest concentrations, in the low ng/m^3 range. Nearly all trace elements were present in higher concentrations in Nógrádmegyer. The highest mean concentrations for almost all elements occurred during the heating period, likely due to factors such as low ambient temperatures, and a deeper mixing layer. The trace elements appeared to fall into three groups based on their seasonal variability. The first group includes As, Cd, Co, Cr, Ni, Pb, Sb, and Zn, which showed higher mean concentrations during the heating period. These elements are likely associated with coal, waste, wood combustion, and traffic emissions (Dung et al., 2018; Pulong et al., 2017). The second group includes Ba and Fe, which presented higher mean concentrations during the non-heating period, linked to both natural and anthropogenic sources (Wang et al., 2015). The third group comprises elements such as Cu, Mn, Sn, Sr, and Ti, for which seasonal variability was either not statistically significant or unclear across the two sites. Similar to other air pollutants, trace element concentrations were generally higher in Nógrádmegyer, except for Mn. The International Agency for Research on Cancer (IARC) has classified Pb, Ni, Cd, and As as Group 1 carcinogens (IARC, 2016). According to the air quality standards set by the European Commission, the yearly mean limit values for Cd, Ni, As, and Pb are 5, 20, 6 and 500 ng/m^3 , respectively. While As, Ni, and Pb remained below these limits, Cd concentrations exceeded the yearly mean limit value in both urban and rural areas during the heating period.

3.2.7. Volatile organic compounds and carbonyls

Among the investigated VOCs, benzene was present in the highest concentrations with a mean value of 3.95 and 0.91 $\mu\text{g}/\text{m}^3$ in the heating and non-heating periods, respectively. It was followed by toluene, which had mean values of 1.69 and 1.16 $\mu\text{g}/\text{m}^3$ in the heating and non-heating periods, respectively. Ethylbenzene and styrene were measured at lower

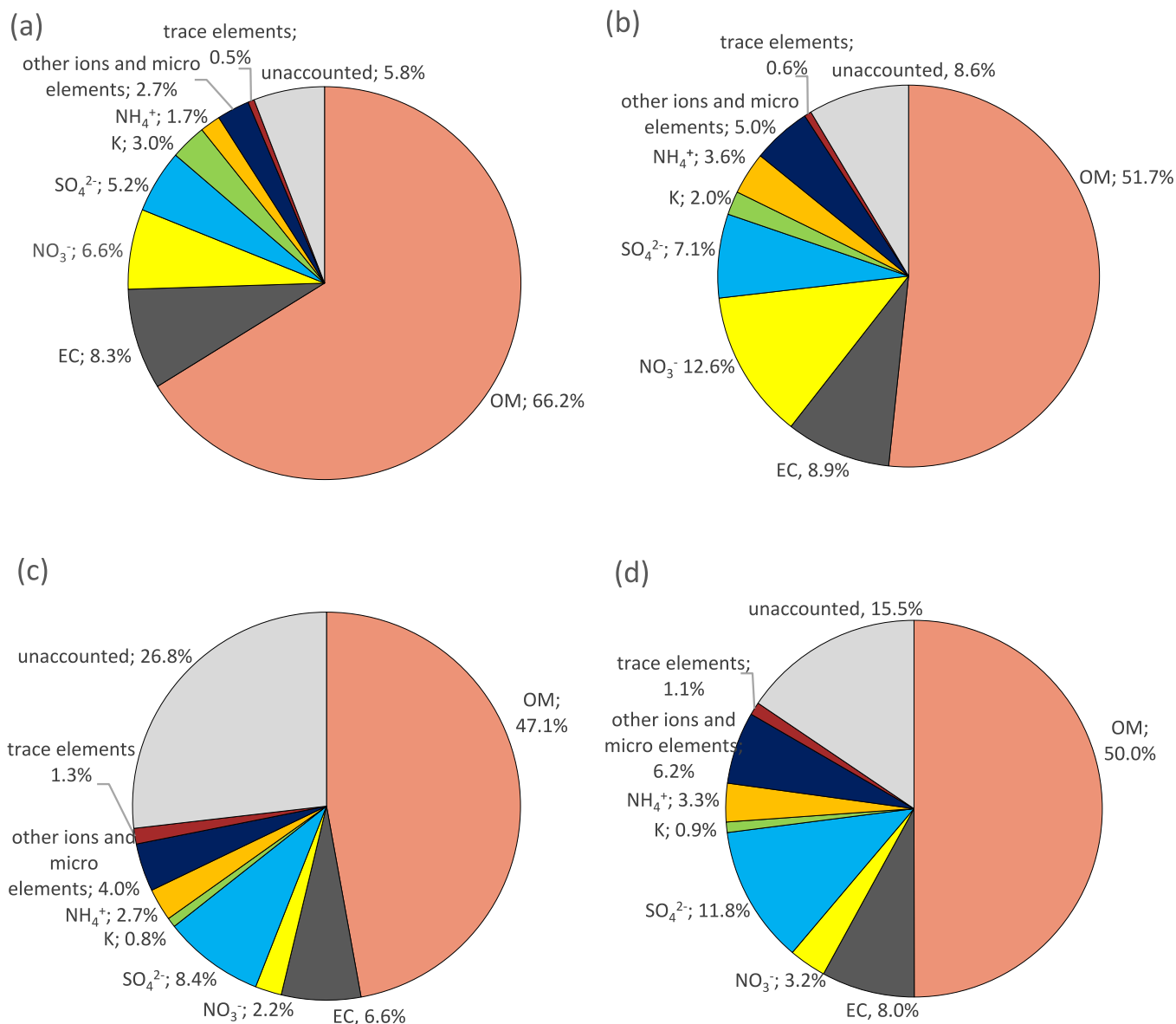


Fig. 2. Mass closure (expressed in %) of $PM_{2.5}$ for (a) rural site - heating period; (b) urban site - heating period; (c) rural site - non-heating period and (d) urban site - non-heating-period. Abbreviations: OM = organic matter; EC = elemental carbon; other ions and micro elements = Na, Ca, Mg, Cl^- .

concentrations, both showing a maximum in the heating period in both settlements. At the lowest concentrations, possible marker compounds of plastic combustion, such as cyclopentanone, allylbenzene, and decane (Sacco et al., 2019), were detected, with concentration values below the LOQ. The concentrations of VOCs were generally higher at the rural site than at the urban site. In Nógrádmegyer, the mean values for benzene, toluene, m + p-xylene, and ethylbenzene were 3.44, 1.58, 1.46 and 0.50 $\mu\text{g}/\text{m}^3$, respectively. In contrast, the corresponding mean values were 1.42, 1.27, 0.90 and 0.48 $\mu\text{g}/\text{m}^3$ for benzene, toluene, m + p-xylene and for ethylbenzene in Esztergom, respectively. Some studies have highlighted benzene, toluene, ethylbenzene, xylenes (BTEX) compounds as one of the primary products of residential wood combustion (Evtyugina et al., 2013; Hellén et al., 2006). In Nógrádmegyer, BTEX compound concentrations were 2–3 times higher than those measured in Esztergom. Specifically, the concentrations of benzene, toluene, and ethylbenzene were 2.9, 1.8, and 1.3 times higher in Nógrádmegyer compared to those measured for the samples collected in Esztergom, respectively.

Among the investigated carbonyls, formaldehyde and acetaldehyde were the most abundant compounds. The mean concentrations of formaldehyde and acetaldehyde were 4.64 and 3.04 $\mu\text{g}/\text{m}^3$ in Nógrádmegyer, and 2.47 and 3.64 $\mu\text{g}/\text{m}^3$ in Esztergom for the heating period, respectively. While previous studies have highlighted the significant emission of aldehydes, particularly formaldehyde and acetaldehyde, from residential BB activities (Cerqueira et al., 2013; Gustafson et al., 2007; Hedberg et al., 2002; Hellén et al., 2006), the results of our study do not conclusively support a dominant contribution from BB to aldehyde levels in the investigated areas. Furthermore, formaldehyde and acetaldehyde consistently exhibit the highest concentrations among measured components in outdoor environments, regardless of the season, suggesting that their presence may be influenced by a range of sources beyond residential BB.

Table 2

Spearman's rank correlation coefficients between PM_{2.5} mass concentration and several meteorological parameters.

	Heating period	Non-heating period
Rural site (Nógrádmegyer)		
Temperature (°C)	-0.44 (p = 0.11)	0.84 (p < 0.01)
Wind speed (m/s)	-0.56 (p < 0.05)	-0.37 (p = 0.19)
Relative humidity (%)	-0.10 (p = 0.74)	-0.50 (p = 0.07)
Pressure (hPa)	0.52 (p = 0.08)	-0.51 (p = 0.09)
Boundary layer height (m)	-0.53 (p = 0.05)	0.21 (p = 0.47)
Urban site (Esztergom)		
Temperature (°C)	-0.45 (p = 0.11)	0.72 (p < 0.01)
Wind speed (m/s)	-0.58 (p < 0.05)	-0.54 (p = 0.05)
Relative humidity (%)	-0.04 (p = 0.90)	-0.62 (p < 0.05)
Pressure (hPa)	0.53 (p = 0.05)	-0.06 (p = 0.85)
Boundary layer height (m)	-0.78 (p < 0.01)	0.01 (p = 0.97)

3.3. Chemical mass closure

Fig. 2 shows the relative contribution of various constituents to the PM_{2.5} mass concentration during the heating and non-heating periods at both settlements. The conversion of OC to OM is recognised as one of the primary sources of uncertainty in chemical mass closure calculations. A conversion factor of 1.4 is commonly applied for both urban and rural areas (Putaud et al., 2004; Sillanpää et al., 2006). However, using a single factor across all sites may introduce uncertainties, as source contributions vary by location and season. OM tends to be more oxidised in rural areas, which generally leads to a higher conversion factor (Turpin and Lim, 2001). Reviewing conversion factors from the literature, Turpin and Lim (2001) recommended 1.6 ± 0.2 for urban areas and $1.6\text{--}2.1 \pm 0.2$ for non-urban areas. Experimentally derived conversion factors for the rural background site K-pusztá in Hungary range from 1.9 to 2.0 (Kiss et al., 2002), while factors of 1.95–2.05 were reported for suburban and rural sites (Bressi et al., 2013). For this study, we applied an OC to OM conversion factor of 1.6 for the urban site and 1.9 for the rural site throughout the campaigns. OM constituted a significant fraction of PM_{2.5} at both sites, accounting for an average of 56.7% at the rural site and 50.9% at the urban site, with higher contributions observed during the heating period. EC contributed moderately to PM_{2.5}, with average values of 7.5% at the rural site and 8.5% at the urban site. In addition to carbonaceous fractions, water soluble ions and micro elements (SO₄²⁻, NO₃⁻, NH₄⁺, K, and others) made up a substantial portion of PM_{2.5}, averaging 18.6 and 27.8% at the rural and urban sites, respectively. Among the water-soluble ions, NO₃⁻ was dominant in the heating period and SO₄²⁻ in the non-heating period at both sites, contributing approximately 10% to PM_{2.5}. Seasonal variations in ion concentrations are largely driven by meteorological factors - such as temperature, relative humidity, and wind speed - which can either facilitate or hinder pollutant dispersion. Regarding the chemical composition, it is noteworthy that, on average, 85% of the PM_{2.5} fraction collected on quartz filters could be identified. The remaining unidentified mass likely includes aerosol-bound water, unanalysed components (e.g. non-soluble crustal elements), and random or systematic errors, including uncertainty in the OM conversion factor (Putaud et al., 2004; Sillanpää et al., 2006). The fraction of unaccounted mass was considerably higher during the non-heating period, consistent with other studies that reported greater unidentified mass in summer than in winter (Cheung et al., 2011). A study on PM water content found seasonal variability, with higher water content in warmer months (Hueglin et al., 2005), suggesting that the increased water content in summer may contribute to the higher unidentified fraction. Overall, this chemical composition aligns with findings from other European studies (Putaud et al., 2010).

4. Discussion

4.1. Relationship between PM_{2.5} and meteorological parameters

To investigate the association between PM_{2.5} mass concentration and meteorological parameters, Spearman's rank correlation coefficients were produced using daily mean values of temperature, wind speed, relative humidity, atmospheric pressure, PBL height, and PM_{2.5} mass concentrations (Table 2). While the association between meteorological parameters and PM_{2.5} mass concentration is inherently complex, some significant associations were identified, particularly with PBL height, temperature, and wind speed. The seasonality of these associations was analysed separately, revealing considerable differences between the heating and non-heating periods. In the non-heating period, temperature showed a positive association with PM_{2.5} mass concentration. This pattern suggests that, in summer, slightly elevated PM_{2.5} mass concentrations at higher temperatures may be linked to enhanced secondary aerosol formation under more intense photochemical activity. In the heating period, wind speed and PBL height were negatively and significantly associated with PM_{2.5} mass concentrations. Although temperature also showed a negative association during this period, it was statistically not significant. These patterns likely reflect increased emissions from residential solid fuel combustion (e.g. wood and coal) combined with reduced atmospheric dispersion under cold, stable conditions that suppress convection. The negative association between PM_{2.5} and PBL height underscores the limited vertical mixing during winter, which contributes to air pollution episodes. Regarding relative humidity, the associations were negative for both periods, with stronger associations for the non-heating period. These findings indicate that meteorological conditions influence PM_{2.5} concentrations differently depending on the season, while changes in the concentration ratios of the pollutants are more indicative of shifts in emission sources. Ferenczi et al. (2021) reported similar associations for temperature and PBL height in Hungary, supporting the robustness of these observations.

4.2. Markers of solid fuel combustion

4.2.1. Spatial and temporal variability

a) Wood burning markers

Residential wood combustion has been identified as a significant source of air pollution in various urban and rural areas across numerous European countries, including Austria (Caseiro et al., 2009), Belgium (Maenhaut et al., 2012), the Czech Republic (Cigánková et al., 2021), France (Favez et al., 2009), Hungary (Salma et al., 2017), Italy (Piazalunga et al., 2011), Portugal (Amato et al., 2016), Romania (Marmureanu et al., 2020), and Switzerland (Szidat et al., 2009). The marker/tracer method relies on the identification of markers directly related to wood burning emissions, enabling the estimation of BB contributions to PM mass concentrations.

LEV and its isomers have been recognised as suitable markers for BB, and more specifically for wood burning, due to their abundance and stability, which are superior to those of other organic tracers (Bhattacharai et al., 2019). During the heating period, the mean concentrations of LEV, MAN, and GAL were 1.5, 1.1, and 1.3 times higher, respectively, in Nógrádmegyer than in Esztergom. BB is more common in rural settlements, which may explain these higher concentrations. A pronounced seasonal variation was observed, with LEV concentrations during the heating period being, on average, 30 times higher than during the non-heating period, which is consistent with findings across Europe. Several studies have reported that LEV concentrations in winter can exceed summer levels by more than a factor of 20 (Puxbaum et al., 2007; Yttri et al., 2005; Zdráhal et al., 2002). The heating/non-heating period concentration ratios for MAN and GAL were 7.2 and 7.9, respectively. The MAs detected during summer likely originate from intermittent twig

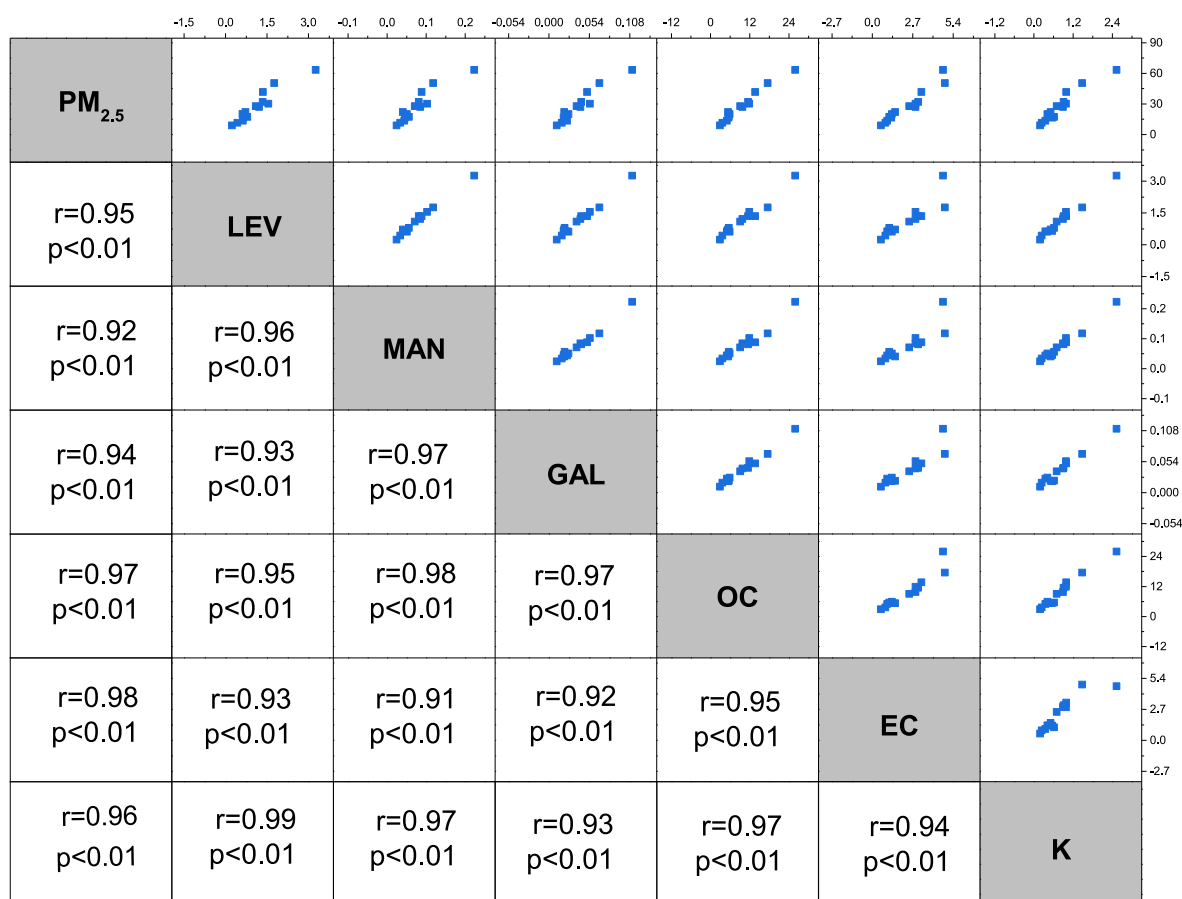


Fig. 3. Scatter plots and Spearman's rank correlation coefficients between the concentrations of PM_{2.5} mass, monosaccharide anhydrides (LEV, MAN, GAL), organic carbon (OC), elemental carbon (EC) and potassium (K) in N6gr6dmgygy during the heating period.

and leaf litter burning as well as wood fire cooking. Nevertheless, their concentrations exhibit a marked seasonal variation, peaking in winter, which suggest that residential wood burning intensifies during colder months.

MA concentrations measured in both settlements were 1.5–2 times higher compared to those obtained in other studies carried out in the Carpathian Basin (Blumberger et al., 2019; Salma et al., 2017, 2020). While the mean LEV concentration at the urban site was comparable to levels reported in other European cities, the mean LEV concentration at the rural site was about 50% higher than previously reported for urban and rural locations across Europe during heating periods (Bari et al., 2010; Caseiro et al., 2009; Glasius et al., 2008; Hedberg et al., 2002; Janoszka et al., 2020, 2022; Kr6mal et al., 2010; Maenhaut et al., 2012, 2016; Piazzalunga et al., 2011; Schwarz et al., 2016; Szidat et al., 2009; Yttri et al., 2005). This is likely due to the fact that we selected a municipality where solid fuels are widely used for both heating and cooking.

K is frequently used as an inorganic tracer to estimate BB contributions to ambient PM, due to the presence of potassium oxide and salts in wood smoke (Chen et al., 2017; Galindo et al., 2021). However, K is not exclusive to biomass combustion, as other sources, such as soil dust, fertilizers, industrial emissions, sea spray, and volcanic activity, also contribute to K levels (Pachon et al., 2013). In our study, K concentrations at the rural site were more than three times higher than those measured by Salma et al. (2020) at K-puszta (a rural background site) in winter 2018. The elevated K concentrations during cold periods are attributed to wood burning associated with residential heating. The concentrations at the urban site were similar to those reported for various locations within the Carpathian Basin (Szidat et al., 2009; Schwarz et al., 2016; Maenhaut et al., 2016).

Using well-established tracers, such as LEV, we observed associations between LEV and other pollutants known to be co-emitted during wood burning. As shown in Fig. 3, the concentrations of PM_{2.5}, LEV, MAN, GAL, OC, EC, and K were strongly correlated ($r > 0.91$) during the heating period for the rural site. This coherence suggests that these species likely originate from a common source, specifically residential wood burning, which is consistent with findings from earlier studies. Similar associations were found for the urban site (Figure A.1).

Several studies have shown that residential wood burning is a significant source of airborne PAHs, particularly BaP (Glasius et al., 2008; Guerreiro et al., 2015; Hell6n et al., 2008; Silibello et al., 2012). BaP is commonly used as a marker for both total and carcinogenic PAHs (EU Directive, 2004). A European directive has set a target value of 1 ng/m³ for the total BaP content in the PM₁₀, averaged over a calendar year (EU Directive, 2004). A reference level of 0.12 ng/m³ was established based on the WHO unit risk for lung cancer due to PAH mixtures, with an acceptable risk of additional lifetime cancer risk of approximately 1×10^{-5} (ETC/ACM, 2011). Our results indicate that relatively high BaP concentrations were detected in PM_{2.5} samples, especially in N6gr6dmgygy. The BaP concentration exceeded the annual target value of 1 ng/m³ in 100% of samples from N6gr6dmgygy and in 64% of samples from Esztergom during the heating period. During one of the heating period's measurement days, the BaP concentration reached 13.2 ng/m³ in N6gr6dmgygy, exceeding the annual target value by an order of magnitude. The WHO reference level of 0.12 ng/m³ for BaP was surpassed daily at both monitoring sites. Concentrations of PAHs, including BaP, in ambient air are a significant concern in Europe, as levels have frequently exceeded target values (EEA, 2022). Considering the WHO reference level, it is estimated that 90% of the urban population in the EU is exposed to BaP levels above the acceptable reference

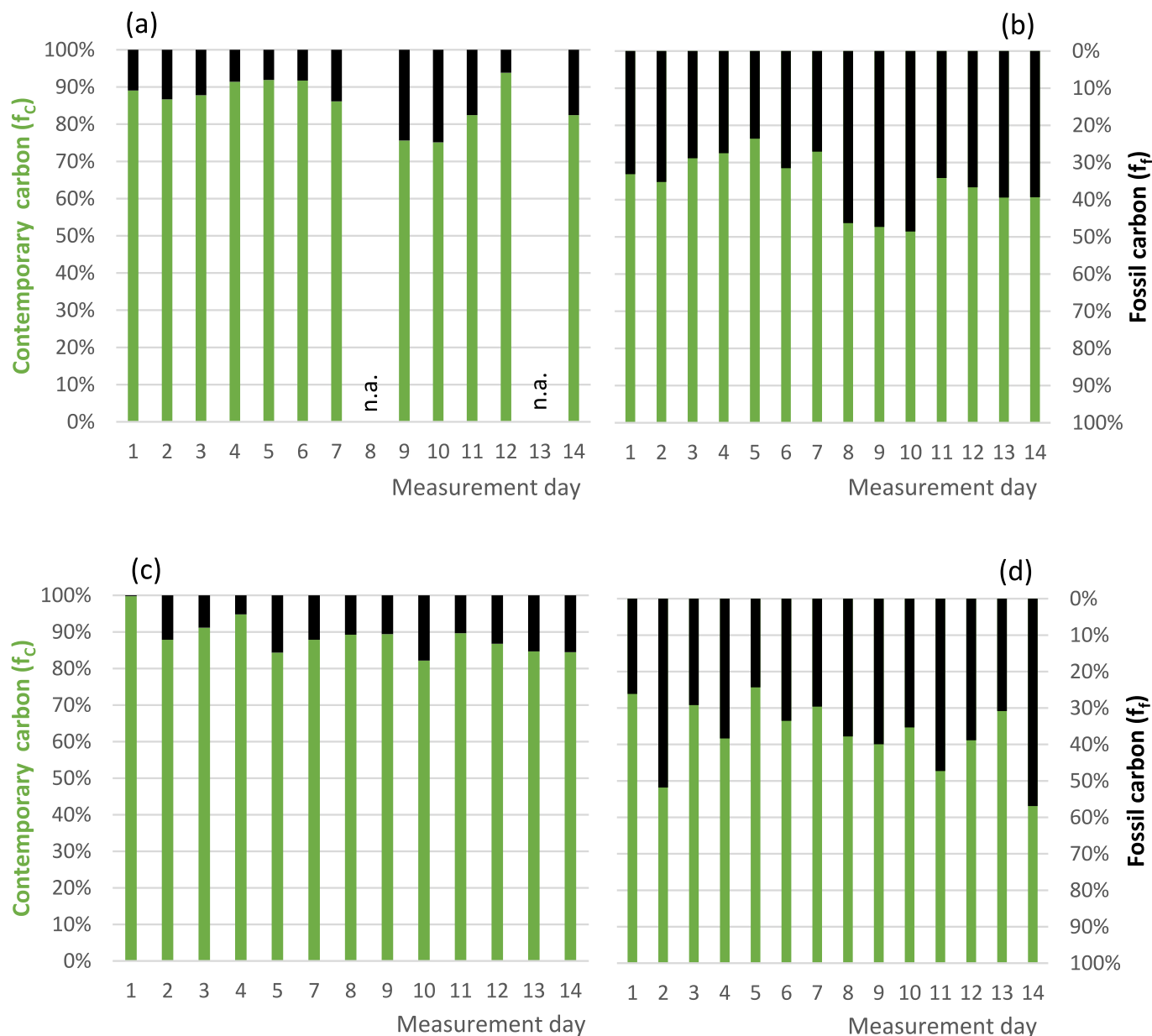


Fig. 4. The distribution ratio between contemporary (f_c) and fossil carbon (f_f) in the PM_{2.5} during the study period (a) urban site - heating period; (b) urban site - non-heating period; (c) rural site - heating period; (d) rural site - non-heating period. Abbreviation: n.a = not available.

level (EEA, 2015).

The ^{14}C measurement has proved to be a powerful and valuable tool for narrowing down the potential sources. ^{14}C is a unique tracer in the source apportionment of atmospheric carbonaceous particles, as ^{14}C measurements enable a distinction between modern or contemporary carbon and fossil carbon origin. Fig. 4 shows the variation of contemporary/fossil carbon ratios (f_c/f_f) within the TC content, based on the ^{14}C measurements. The distinction between contemporary and fossil carbon is particularly relevant in understanding seasonal changes. Contemporary carbon includes both natural and anthropogenic sources, while fossil carbon is almost exclusively anthropogenic. During the heating period, the intensity of natural carbon sources decreases, while the amount of contemporary carbon from anthropogenic sources increases. This can be attributed to residential heating being a primary source of carbon during the winter. In the case of coal and oil combustion, an aerosol containing fossil carbon is formed, while in the case of

wood burning, an aerosol containing contemporary carbon is formed. During the heating period, the share of contemporary carbon peaked, while the contribution of fossil carbon was at its lowest. This indicates that the main source of the carbon during the heating period is primarily of contemporary origin, most likely from residential wood burning by the inhabitants.

During the non-heating period, the share of contemporary carbon decreases relative to fossil carbon. In summer, the influence of wood fire cooking and increased biological activity from vegetation becomes more significant, while residential heating is negligible. Consequently, the contribution of contemporary carbon primarily arises from the release of primary aerosols and secondary organic aerosol precursors from vegetation, along with the burning of agricultural crops and burning of green waste in residential areas. The mass concentration of fossil-derived PM_{2.5} in the non-heating period is approximately twice that observed in the heating period. This suggests that, despite increased biogenic

activity, fossil fuel combustion from traffic and other activities was a dominant source at both sites during the non-heating period. Changes in the contemporary/fossil carbon ratio are more likely to be driven by the significant increase of BB during the heating season and its rapid decline in the spring. The higher concentration of fossil-derived particles during the non-heating period is likely due to the synergistic effects of multiple anthropogenic sources. These findings are consistent with previous observations in Hungary (Gelencsér et al., 2007; Major et al., 2015, 2021) and other European cities (Szidat et al., 2009; Kontul et al., 2020).

To investigate the association between the concentrations of contemporary carbon and tracers of BB (LEV, OC, EC, TC, K, PM_{2.5}), Spearman's rank correlation coefficients were calculated for both sampling sites during the heating period. At the urban site, the contemporary carbon concentrations showed strong and statistically significant positive associations with all markers supporting BB as the dominant source of contemporary carbon. In contrast, at the rural site, associations between the concentrations of contemporary carbon and the same markers were weak and statistically not significant. These findings suggest that, in addition to BB, other non-fossil contemporary carbon sources contributed substantially to the PM_{2.5} composition at the rural site. One potential source is the combustion of mixed household organic waste (such as food scraps, paper, textiles), which has been identified in rural Hungarian settings based on chemical marker analysis (Hoffer et al., 2024). Although these materials are of non-fossil origin, they may not emit the same marker compounds typically used to trace BB, potentially explaining the low correlations observed. This interpretation is supported by the LEV/TC concentration ratios, which were found to be slightly higher at the urban site (mean: 0.109) than at the rural site (mean: 0.095), suggesting marginally lower BB contributions at the rural site.

b) Waste burning markers

Although household waste burning is legally prohibited in Hungary, evidence suggests that residents may still burn waste for heating purposes (e.g. Kantar Hoffman, 2017; Századvég Foundation, 2018). 135-TPB has been proposed as a distinctive tracer for waste burning emissions (Simoneit et al., 2005). The combustion of polyethylene (PE), polyethylene terephthalate (PET), and mixed waste produces substantial amounts of 135-TPB and, to a lesser extent, 124-TPB (Simoneit, 2015; Simoneit et al., 2005; Tomsej et al., 2018). The presence of these compounds in ambient PM_{2.5} may indicate illegal waste burning. Recent research supports the use of 135-TPB as an effective marker for PET combustion in air quality monitoring (Furman et al., 2021) and it has been applied as a universal tracer for waste burning in several studies (Hoffer et al., 2021; Simoneit, 2015; Simoneit et al., 2005; Tomsej et al., 2018). In our study, 135-TPB was detected in 93% of PM_{2.5} samples collected in Nógrádmegyer and in 64% of samples from Esztergom during the heating period. The mean concentration of 135-TPB was notably higher in Esztergom (0.77 ng/m³) compared to Nógrádmegyer (0.43 ng/m³) during the heating period, although the median concentration was higher in Nógrádmegyer (0.32 ng/m³) than in Esztergom (0.15 ng/m³). This discrepancy is due to an exceptionally high maximum value recorded on the final day in Esztergom, which was approximately 30 times higher than the results obtained for the other days, and significantly skewed the overall mean value. During the non-heating period, 135-TPB was frequently below the LOD. In addition to 135-TPB, its structural isomer 124-TPB was detected exclusively at the Nógrádmegyer site, with quantifiable concentrations on four measurement days during the heating period and one day during the non-heating period. Several studies have reported 135-TPB concentrations in PM₁₀ samples (Hoffer et al., 2024; Hoffer et al., 2021; Furman et al., 2021; Simoneit et al., 2005). Concentration levels in this study were lower than those observed in Romania during winter 2020 (2.7–3.6 ng/m³, Hoffer et al., 2021) and in Wadowice, Poland, during the heating season of 2017 (0.8 ng/m³, Furman et al., 2021), but slightly

higher than results obtained in Hungary in winter 2018 (Hoffer et al., 2024). In Hungary, the mean atmospheric concentrations of 135-TPB in PM₁₀ samples were ranged between 0.25 and 0.42 ng/m³ across different sampling stations (Hoffer et al., 2024). The successful detection of 135-TPB in atmospheric PM samples reinforces its potential as a reliable marker for monitoring residential waste combustion, particularly during the heating season.

Significant metal emissions are also expected from waste burning, as waste materials generally contain higher metal content than conventional fuels. Antimony is linked to plastic and municipal waste incineration but also originates from traffic, as brake linings containing 1–5% stibnite (Sb₂S₃) release it during wear (Roubicek et al., 2008). Waste incineration emissions may also include trace elements, such as As, Cd, Co, Cr, Ni, Pb, and Zn (Dung et al., 2018), some of which are also associated with transportation activities, such as resuspended road dust and the wear of vehicle components. According to the Biomass Energy Centre, untreated wood typically contains very low levels of heavy metals; however, wood treated with preservatives or coatings can contain significant levels (Biomass Energy Centre, 2012). For example, wood used outdoors is often treated with chromate copper arsenate. If burned inappropriately, such wood can release As, Co and Cr into the atmosphere.

Associations between trace element concentrations and BB markers were examined at both sites and during both periods; however, no significant associations were found. To further explore potential sources, associations between the concentrations of 135-TPB and trace elements were investigated. Moderate to strong associations were found for some trace elements at both locations (rural site: Ba, Zn, Cd, Sb; urban site: Co, Pb, Sb, Ni, Cu, Fe, V). Due to the overlapping origins of many trace elements, source attribution remains uncertain and should be interpreted with caution. At the rural site, the observed associations, along with the considerably higher concentrations of Zn and Sb, and more consistent with emissions from the burning of mixed household waste. In contrast, at the urban site, traffic-related sources likely play a more prominent role, with additional contributions from waste burning and industrial combustion also possible.

4.2.2. Contribution of different sources to PM mass

Several studies have utilised the LEV/PM concentration ratio to estimate the contribution of wood burning emissions to ambient aerosols (Galindo et al., 2021; Schmidl et al., 2008; Janoszka and Czaplicka, 2022). Evidence of wood burning contributions to PM_{2.5} was observed at both settlements. These contributions were higher during colder months in both cities, consistent with increased residential wood combustion. The magnitude of wood burning emissions was similar at the investigated sites, with mean LEV/PM concentration ratios of 0.04 and 0.046 in Nógrádmegyer and Esztergom, respectively.

While all three MAs derive from biomass combustion, their relative proportions depend on the type of biofuel burned. The LEV/MAN concentration ratio helps identify the type of wood being burned, with lower ratios (approx. 3) indicating softwoods like pine, and higher ratios (14–15) indicating hardwoods like oak and beech (Schmidl et al., 2008). In our samples, the mean LEV/MAN concentration ratio was 14.3 at the rural site and 10.7 at the urban site, suggesting predominantly hardwood combustion in Nógrádmegyer and mixed wood use in Esztergom.

The LEV/(MAN + GAL) concentration ratio can help distinguish wood burning from other BB emissions. Typical values reported in the literature are >50 for lignite, 2.5 for coal, 5 for peat, 8.5–9.9 for hardwood, and 1.2–2.8 for softwood (Fabbri et al., 2009; Schmidl et al., 2008). In our study, the mean LEV/(MAN + GAL) concentration ratios were 9.6 in Nógrádmegyer and 7.3 in Esztergom, consistent with hardwood combustion.

According to the literature, a high OC/EC concentration ratio is indicative of combustion from heating sources, such as solid fuel combustion. Typical values are 4.2 for wood burning, 12.7 for natural gas, and 2.6–6.0 for coal. In contrast, low OC/EC concentration ratios are

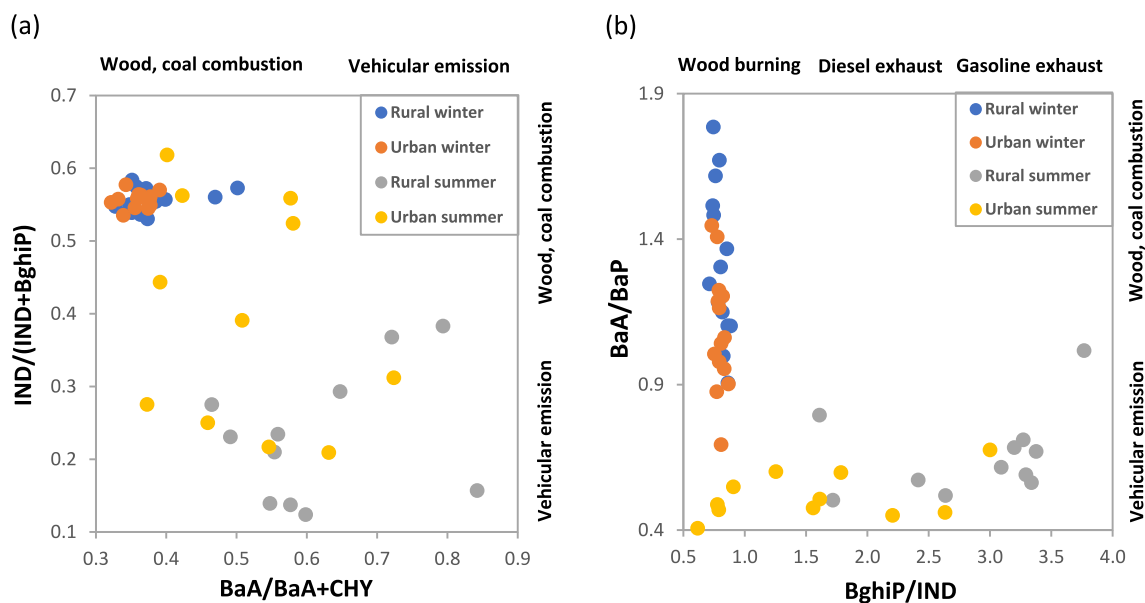


Fig. 5. Results of PAH diagnostic ratios (a) $BaA/(BaA + CHY)$ and $IND/(IND + BghiP)$ (b) $BghiP/IND$ and BaA/BaP . Rural: Nógrádmegyer, Urban: Esztergom, winter: heating period, summer: non-heating period.

associated with vehicular emissions, such as 2.2 for gasoline and 0.8 for diesel emissions (Na et al., 2004). In Esztergom, OC/EC concentration ratios ranged from 2.2 to 10.2 (mean: 4.2), while in Nógrádmegyer, the range was 1.8–7.7 (mean: 4.2) for all samples. The high ratios suggest local sources, such as wood and coal combustion. During the heating period, the mean OC/EC concentration ratios were 3.8 in the urban area and 4.3 in the rural area, while in the non-heating period, they were 4.6 and 4.1, respectively. In Esztergom, the summer maximum could be linked to increased photochemical activity, whereas in Nógrádmegyer, the winter maximum likely results from elevated residential heating.

Diagnostic ratios based on the relative abundance of individual PAHs are widely used to identify emission sources. Previous studies have found specific PAH species associated with combustion and traffic sources. Six common diagnostic ratios were investigated: $IND/(IND + BghiP)$, $BaP/(BaP + CHY)$, $BaA/(BaA + CHY)$, $FLT/(FLT + PYR)$, $BghiP/IND$, and BaA/BaP . In this study, Fig. 5 presents the distribution of these diagnostic ratios across rural (Nógrádmegyer) and urban (Esztergom) sites. Ratios below 0.5 for $IND/(IND + BghiP)$ suggest vehicular emissions, while values above 0.5 indicate coal and wood combustion (Ravindra et al., 2008). In this study, the $IND/(IND + BghiP)$ concentration ratios of 0.56 at the rural site and 0.55 at the urban site indicate a dominant influence of wood and coal combustion (Yunker et al., 2002). A $BaP/(BaP + CHY)$ concentration ratio of 0.31 in Nógrádmegyer and 0.35 in Esztergom also suggests solid fuel combustion (Rogge et al., 1998). The $FLT/(FLT + PYR)$ concentration ratio exceeded 0.4, indicating mixed coal and biomass combustion sources (Yunker et al., 2002; De Zárate et al., 2000). During summer, PAH ratios indicated the influence of traffic emissions, particularly diesel in Esztergom and potentially gasoline in Nógrádmegyer.

The benzene/toluene concentration ratio is another indicator used to identify emission sources. Ratios around 2.2 suggest residential wood heating, while values near 0.3 are typical of traffic emissions (Hellén et al., 2006). In our study, the benzene/toluene concentration ratio averaged 2.2 in Nógrádmegyer, indicative of wood burning, and 1.1 in Esztergom, suggesting a mix of traffic and wood combustion influences.

5. Conclusions

Solid fuels remain widely used for residential heating, significantly affecting air quality by emitting fine particles and other pollutants. Within this study, we analysed several specific markers associated with residential solid fuel combustion, confirming its considerable impact on air quality in both rural and urban areas. Air pollutant concentrations increased notably during the heating period. Besides the high concentrations of BB markers, the detection of 135-TPB indicates that waste burning may also occur, despite legal prohibitions. Residential solid fuel combustion poses serious health risks, as it produces higher concentrations of $PM_{2.5}$ and hazardous substances compared to other heating methods. Correlation analysis revealed that $PM_{2.5}$ levels during the heating period were highest under conditions of low temperatures, reduced PBL height, and calm or stagnant air, all of which contribute to increased pollution. While long-term solutions involve transitioning to renewable energy and modernising heating systems, immediate actions can help mitigate the impacts of solid fuel combustion. Encouraging a shift from solid fuels, adopting cleaner technologies, and increasing public awareness through targeted campaigns are essential steps. National air quality programmes should prioritise reducing residential solid fuel combustion and implement strategies to prevent illegal waste burning, thus safeguarding public health.

CRedit authorship contribution statement

Boglárka S. Balogh: Writing – original draft, Project administration, Methodology, Investigation, Data curation. **Zsófia Csáková:** Writing – review & editing, Investigation, Data curation. **Zoltán Nyiri:** Writing – review & editing, Investigation, Data curation. **Balázs Berlinger:** Writing – review & editing, Investigation, Data curation. **Mihály Molnár:** Writing – review & editing, Investigation, Data curation. **István Major:** Writing – review & editing, Investigation, Data curation. **Virág Gergely:** Writing – review & editing, Investigation, Data curation. **Tamás Szigeti:** Writing – review & editing, Supervision, Investigation, Conceptualization.

Declaration of competing interest

The authors declare that they have no known competing financial interests or personal relationships that could have appeared to influence the work reported in this paper.

Acknowledgement

The assistance of Gábor Rési (NCPHP) in the sample collection is warmly thanked. István Major was supported by the János Bolyai Research Scholarship of the Hungarian Academy of Sciences (BO/00710/23/10).

Appendix A. Supplementary data

Supplementary data to this article can be found online at <https://doi.org/10.1016/j.atmosenv.2025.121399>.

Data availability

Data will be made available on request.

References

- Amato, F., Alastuey, A., Karanasiou, A., Lucarelli, F., Nava, S., Calzolari, G., Severi, M., Becagli, S., Gianelle, V.L., Colombi, C., Alves, C., Custódio, D., Nunes, T., Cerqueira, M., Pio, C., Eleftheriadis, K., Diapouli, E., Reche, C., Minguillón, M.C., Manousakas, M.I., Maggos, T., Vratolis, S., Harrison, R.M., Querol, X., 2016. AIRUSE-LIFE+: a harmonized PM speciation and source apportionment in five southern European cities. *Atmos. Chem. Phys.* 16, 3289–3309. <https://doi.org/10.5194/acp-16-3289-2016>.
- Angyal, A., Szoboszlai, Z., Major, I., et al., 2024. Characterisation of urban aerosol size distribution by radiocarbon and PIXE analyses in a middle-European urban environment for source identification: a pilot study. *Environ. Sci. Pollut. Res.* 31, 47258–47274. <https://doi.org/10.1007/s11356-024-34215-8>.
- Balmes, J.R., 2019. Household air pollution from domestic combustion of solid fuels and health. *J. Allergy Clin. Immunol.* 143 (6), 1979–1987. <https://doi.org/10.1016/j.jaci.2019.04.016>.
- Bari, M.A., Baumbach, G., Kuch, B., Scheffknecht, G., 2010. Particle-phase concentrations of polycyclic aromatic hydrocarbons in ambient air of rural residential areas in southern Germany. *Air Qual. Atmos. Health* 3, 103–116. <https://doi.org/10.1007/s11869-009-0057-8>.
- Bhattarai, H., Saikawa, E., Wan, X., Zhu, H., Ram, K., Gao, S., Kang, S., Zhang, Q., Zhang, Y., Wu, G., Wang, X., Kawamura, K., Fu, P., Cong, Z., 2019. Levoglucosan as a tracer of biomass burning: recent progress and perspectives. *Atmos. Res.* 220, 20–33. <https://doi.org/10.1016/j.atmosres.2019.01.004>.
- Biomass Energy Centre, 2012. Wood as fuel: A guide to choosing and drying logs. Forestry Commission, UK. Available at: https://cdn.forestresearch.gov.uk/2022/02/fr-bec-wood-as-fuel_v2.pdf.
- Blumberger, Z.I., Vasanits-Zsigrai, A., Farkas, G., Salma, I., 2019. Mass size distribution of major monosaccharide anhydrides and mass contribution of biomass burning. *Atmos. Res.* 220, 1–9. <https://doi.org/10.1016/j.atmosres.2019.01.001>.
- Braníš, M., Domasová, M., 2003. PM₁₀ and black smoke in a small settlement: case study from the Czech Republic. *Atmos. Environ.* 37 (1), 83–92. [https://doi.org/10.1016/S1352-2310\(02\)00700-8](https://doi.org/10.1016/S1352-2310(02)00700-8).
- Bressi, M., Sciare, J., Ghersi, V., Bonnaire, N., Nicolas, J.B., Petit, J.E., Moukhtar, S., Rosso, A., Mihalopoulos, N., Féron, A., 2013. A one-year comprehensive chemical characterisation of fine aerosol (PM_{2.5}) at urban, suburban and rural background sites in the region of Paris (France). *Atmos. Chem. Phys.* 13, 7825–7844. <https://doi.org/10.5194/acp-13-7825-2013>.
- Caseiro, A., Bauer, H., Schmidl, C., Pio, C.A., Puxbaum, H., 2009. Wood burning impact on PM₁₀ in three Austrian regions. *Atmos. Environ.* 43 (13), 2186–2195. <https://doi.org/10.1016/j.atmosenv.2009.01.012>.
- Cavalli, F., Viana, M., Yttri, K.E., Genberg, J., Putaud, J.-P., 2010. Toward a standardised thermal-optical protocol for measuring atmospheric organic and elemental carbon: The EUSAAR protocol. *Atmos. Meas. Tech.* 3, 79–89. <https://doi.org/10.5194/amt-3-79-2010>.
- Cerqueira, M., Gomes, L., Tarelho, L., Pio, C., 2013. Formaldehyde and acetaldehyde emissions from residential wood combustion in Portugal. *Atmos. Environ.* 72, 171–176. <https://doi.org/10.1016/j.atmosenv.2013.02.045>.
- Chen, Y., Li, X., Zhu, T., Han, Y., Lv, D., 2017. PM_{2.5}-bound PAHs in three indoor and one outdoor air in Beijing: concentration, source and health risk assessment. *Sci. Total Environ.* 586, 255–264. <https://doi.org/10.1016/j.scitotenv.2017.01.214>.
- Cheung, K., Daher, N., Kam, W., Shafer, M.M., Ning, Z., Schauer, J.J., Sioutas, C., 2011. Spatial and temporal variation of chemical composition and mass closure of ambient coarse particulate matter (PM_{10-2.5}) in the Los Angeles Area. *Atmos. Environ.* 45, 2651–2662. <https://doi.org/10.1016/j.atmosenv.2011.02.066>.
- Cigánková, H., Mikuška, P., Hegrová, J., Pokorná, P., Schwarz, J., Krajčovič, J., 2021. Seasonal variation and sources of elements in urban submicron and fine aerosol in Brno, Czech Republic. *Aerosol Air Qual. Res.* 21, 200556. <https://doi.org/10.4209/aaqr.2020.09.0556>.
- Clark, L.M., Peel, J.L., 2013. Health and household air pollution from solid fuel use: the need for improved exposure assessment. *Environ. Health Perspect.* 121, 1120–1128. <https://doi.org/10.1289/ehp.1206429>.
- Dung, T.T.T., Vassiliéva, E., Swennen, R., Cappuyns, V., 2018. Release of trace elements from bottom ash from hazardous waste incinerators. *Recycling* 3, 36. <https://doi.org/10.3390/recycling3030036>.
- ETC/ACM, 2011. Evaluation of current limit and target values as set in the EU Air Quality Directive, de Leeuw, F. and Ruysenaars, P., ETC/ACM Technical Paper 2011/3.
- European Commission, 2004. Directive 2004/107/EC of the European Parliament and of the Council of 15 December 2004 relating to arsenic, cadmium, mercury, nickel and polycyclic aromatic hydrocarbons in ambient air. *Off. J. Eur. Union.* <https://eur-lex.europa.eu/eli/dir/2004/107/oj/eng>.
- European Commission, 2008. Directive 2008/50/EC of the European Parliament and of the Council of 21 May 2008 on ambient air quality and cleaner air for Europe. *Off. J. Eur. Union.* <https://eur-lex.europa.eu/eli/dir/2008/50/oj/eng>.
- European Environment Agency (EEA), 2015. Air quality in Europe — 2015 report. EEA Report No 5/2015, Luxembourg: Publications Office of the European Union. Available at: <https://www.eea.europa.eu/en/analysis/publications/air-quality-in-europe-2015>.
- European Environment Agency (EEA), 2022. Air quality in Europe — 2022 report. EEA Report No 13/2022, Luxembourg: Publications Office of the European Union. Available at: <https://www.eea.europa.eu/publications/air-quality-in-europe-2022>.
- Evtuygina, M., Alves, C., Calvo, A., Nunes, T., Tarelho, L., Duarte, M., Prozil, S.O., Evtuguin, D.V., Pio, C., 2013. VOC emissions from residential combustion of Southern and mid-European woods. *Atmos. Environ.* <https://doi.org/10.1016/j.atmosenv.2013.10.050>.
- Fabbri, D., Torri, C., Simoneit, B.R.T., Marynowski, L., Rushdi, A.I., Fabiańska, M.J., 2009. Levoglucosan and other cellulose and lignin markers in emissions from burning of Miocene lignites. *Atmos. Environ.* 43, 2286–2295. <https://doi.org/10.1016/j.atmosenv.2009.01.030>.
- Favez, O., Cachier, H., Sciare, J., Sarda-Estève, R., Martiñon, L., 2009. Evidence for a significant contribution of wood burning aerosols to PM_{2.5} during the winter season in Paris, France. *Atmos. Environ.* 43, 3640–3644. <https://doi.org/10.1016/j.atmosenv.2009.04.035>.
- Ferenczi, Z., Imre, K., Lakatos, M., Molnár, Á., Bozó, L., Homolya, E., Gelencsér, A., 2021. Long-term characterization of urban PM₁₀ in Hungary. *Aerosol Air Qual. Res.* 21, 210048. <https://doi.org/10.4209/aaqr.210048>.
- Furman, P., Styszko, K., Skiba, A., Zieba, D., Zimnoch, M., Kistler, M., Kasper-Giebl, A., Gilardoni, S., 2021. Seasonal variability of PM₁₀ chemical composition including 1,3,5-triphenylbenzene, marker of plastic combustion and toxicity in Wadowice, South Poland. *Aerosol Air Qual. Res.* 21, 200223. <https://doi.org/10.4209/aaqr.2020.05.0223>.
- Galindo, N., Clemente, A., Yubero, E., Nicolás, J.F., Crespo, J., 2021. PM₁₀ chemical composition at a residential site in the western Mediterranean: estimation of the contribution of biomass burning from levoglucosan and its isomers. *Environ. Res.* 196, 110394. <https://doi.org/10.1016/j.envres.2020.110394>.
- Gelencsér, A., May, B., Simpson, D., Sánchez-Ochoa, A., Kasper-Giebl, A., Puxbaum, H., Caseiro, A., Pio, C., Legrand, M., 2007. Source apportionment of PM_{2.5} organic aerosol over Europe: primary/secondary, natural/anthropogenic, and fossil/biogenic origin. *J. Geophys. Res.* 112, D23S04. <https://doi.org/10.1029/2006JD008094>.
- Gianelle, V., Colombi, C., Caserini, S., Ozgen, S., Galante, S., Marongiu, A., 2013. Benzo(a)pyrene air concentrations and emission inventory in Lombardy region, Italy. *Atmos. Pollut. Res.* 4, 257–266. <https://doi.org/10.5094/APR.2013.029>.
- Glasius, M., Ketzel, M., Wählin, P., Boss, R., Stubkjaer, J., Hertel, O., Palmgren, F., 2008. Characterization of particles from residential wood combustion and modelling of spatial variation in low-strength emission areas. *Atmos. Environ.* 42, 8686–8697. <https://doi.org/10.1016/j.atmosenv.2008.08.016>.
- Guerreiro, C., Horalek, J., de Leeuw, F., Couvidat, F., 2015. Mapping ambient concentrations of benzo(a)pyrene in Europe – population exposure and health effects for 2012. ETC/ACM Technical Paper 2014/6. <https://doi.org/10.13140/RG.2.1.3411.4969>.
- Gustafson, P., Barregard, L., Strandberg, B., Sällsten, G., 2007. The impact of domestic wood burning on personal, indoor and outdoor levels of 1,3-butadiene, benzene, formaldehyde and acetaldehyde. *J. Environ. Monit.* 9, 23–32. <https://doi.org/10.1039/B614142K>.
- Heal, M.R., Naysmith, P., Cook, G.T., Xu, S., Duran, T.R., Harrison, R.M., 2011. Application of 14C analyses to source apportionment of carbonaceous PM_{2.5} in the UK. *Atmos. Environ.* 45, 2341–2348. <https://doi.org/10.1016/j.atmosenv.2011.02.030>.
- Hedberg, E., Kristensson, A., Ohlsson, M., Johansson, C., Johansson, P.A., Swietlicki, E., Vesely, V., Wideqvist, U., Westerholm, R., 2002. Chemical and physical characterization of emissions from birch wood combustion in a wood stove. *Atmos. Environ.* 36, 4823–4837. [https://doi.org/10.1016/S1352-2310\(02\)00417-X](https://doi.org/10.1016/S1352-2310(02)00417-X).
- Hellén, H., Hakola, H., Pirjola, L., Laurila, T., Pystynen, K.H., 2006. Ambient air concentrations, source profiles and source apportionment of 71 different C₂–C₁₀ volatile organic compounds in urban and residential areas of Finland. *Environ. Sci. Technol.* 40, 103–108. <https://doi.org/10.1021/es051431j>.
- Hellén, H., Hakola, H., Pietarila, H., Kauhaniemi, M., Haaparanta, S., 2008. Influence of residential wood combustion on local air quality. *Sci. Total Environ.* 393, 283–290. <https://doi.org/10.1016/j.scitotenv.2008.01.018>.
- Hoffer, A., Tóth, Á., Jancsek-Turóczy, B., Machon, A., Meiravová, A., Nagy, A., Marmureanu, L., Gelencsér, A., 2021. Potential new tracers and their mass fraction

- in the emitted PM₁₀ from the burning of household waste in stoves. *Atmos. Chem. Phys.* 21, 17855–17864. <https://doi.org/10.5194/acp-21-17855-2021>.
- Hoffer, A., Meirav, A., Tóth, A., Jancsek-Turóczy, B., Kiss, G., Rostási, Á., Levei, E.A., Marmureanu, L., Machon, A., Gelencsér, A., 2024. Assessment of the contribution of residential waste burning to ambient PM₁₀ concentrations in Hungary and Romania. *Atmos. Chem. Phys.* 24, 1659–1671. <https://doi.org/10.5194/acp-24-1659-2024>.
- Hueglin, C., Gehrig, R., Baltensperger, U., Gysel, M., Monn, C., Vonmont, H., 2005. Chemical Characterisation of PM_{2.5}, PM₁₀ and Coarse Particles at urban, near-city and rural sites in Switzerland. *Atmos. Environ.* 39, 637–651. <https://doi.org/10.1016/j.atmosenv.2004.10.027>.
- IARC, 2016. Agents classified by the IARC monographs. International Agency for Research on Cancer 1–117. Lyon. <https://monographs.iarc.who.int/agents-classified-by-the-iarc/>.
- Janoszka, K., Czaplicka, M., 2022. Correlation between biomass burning tracers in urban and rural particles in silesia – case study. *Water Air Soil Pollut.* 233, 62. <https://doi.org/10.1007/s11270-022-05523-x>.
- Janoszka, K., Czaplicka, M., Klejnowski, K., 2020. Comparison of biomass burning tracer concentrations between two winter seasons in krynica zdroj. *Air Qual. Atmos. Health* 13, 379–385. <https://doi.org/10.1007/s11869-020-00801-1>.
- Kantar Hoffmann Ltd., 2017. Household waste burning habits in Hungary. https://www.levego.hu/sites/default/files/Kantar_Hoffmann_Levego_MCS_Hulladekegetes_2017dec.pdf (last access: 25 February 2024) (in Hungarian).
- Karagulian, F., et al., 2015. Contributions to cities' ambient particulate matter (PM): a systematic review of local source contributions at global level. *Atmos. Environ.* 120, 475–483. <https://doi.org/10.1016/j.atmosenv.2015.08.087>.
- Kim, K.H., Kabir, E., Kabir, S., 2015. A review on the human health impact of airborne particulate matter. *Environ. Int.* 74, 136–143. <https://doi.org/10.1016/j.envint.2014.10.005>.
- Kiss, G., Varga, B., Galambos, I., Ganszky, I., 2002. Characterization of water-soluble organic matter isolated from atmospheric fine aerosol. *J. Geophys. Res.* 107, 8339. <https://doi.org/10.1029/2001JD000603>.
- Klimont, Z., Kupiainen, K., Heyes, C., Purohit, P., Cofala, J., Rafaj, P., Borken-Kleefeld, J., Schöpp, W., 2017. Global anthropogenic emissions of particulate matter including Black carbon. *Atmos. Chem. Phys.* 17, 8681–8723. <https://doi.org/10.5194/acp-17-8681-2017>.
- Kontul, I., Kaizer, J., Jeskovský, M., Steier, P., Povinec, P.P., 2020. Radiocarbon analysis of carbonaceous aerosols in Bratislava, Slovakia. *J. Environ. Radioact.* 218, 106221. <https://doi.org/10.1016/j.jenvrad.2020.106221>.
- Krugly, E., Martuzevicius, D., Puida, E., Buinevicius, K., Stasiulaitiene, I., Radziuniene, I., Minikauskas, A., Kliucininkas, L., 2014. Characterization of gaseous- and particle-phase emissions from the combustion of biomass-residue-derived fuels in a small residential boiler. *Energy Fuels* 28, 5057–5066. <https://doi.org/10.1021/ef500420t>.
- Křůmal, K., Mikuska, P., Vojtěšek, M., Večeřa, Z., 2010. Seasonal variations of monosaccharide anhydrides in PM₁ and PM_{2.5} aerosol in urban areas. *Atmos. Environ.* 44, 5148–5155. <https://doi.org/10.1016/j.atmosenv.2010.08.022>.
- Lelieveld, J., Evans, J.S., Fnais, M., Giannadaki, D., Pozzer, A., 2015. The contribution of outdoor air pollution sources to premature mortality on a global scale. *Nature* 525, 367–375. <https://doi.org/10.1038/nature15371>.
- Lim, J.H., Park, H.Y., Cho, S.Y., 2021. Evaluation of the ammonia emission sensitivity of secondary inorganic aerosol concentrations measured by the national reference method. *Atmos. Environ.* 270, 118903. <https://doi.org/10.1016/j.atmosenv.2021.118903>.
- Maenhaut, W., Vermeylen, R., Claeys, M., Vercouteren, J., Matheussen, C., Roekens, E., 2012. Assessment of the contribution from wood burning to the PM₁₀ aerosol in Flanders, Belgium. *Sci. Total Environ.* 437, 226–236. <https://doi.org/10.1016/j.scitotenv.2012.08.015>.
- Maenhaut, W., Vermeylen, R., Claeys, M., Vercouteren, J., Roekens, E., 2016. Sources of the PM₁₀ aerosol in Flanders, Belgium, and re-assessment of the contribution from wood burning. *Sci. Total Environ.* 562, 550–560. <https://doi.org/10.1016/j.scitotenv.2016.04.074>.
- Mai, B.X., Qi, S.H., Zeng, E.Y., Yang, Q.S., Zhang, G., Fu, J.M., Sheng, G.Y., Peng, P.N., Wang, Z.S., 2003. Distribution of polycyclic aromatic hydrocarbons in the coastal region of Macao, China: assessment of input sources and transport pathways using compositional analysis. *Environ. Sci. Technol.* 37, 4855–4863. <https://doi.org/10.1021/es034505a>.
- Major, I., Furu, E., Haszpra, L., Kertész, Z., Molnár, M., 2015. One-year-long continuous and synchronous data set of fossil carbon in atmospheric PM_{2.5} and carbon dioxide in Debrecen, Hungary. *Radiocarbon* 57, 991–1002. https://doi.org/10.2458/azu_rc.57.18191.
- Major, I., Furu, E., Varga, T., Horváth, A., Futó, I., Gyökös, B., Somodi, G., Lisztes-Szabo, Zs, Jull, A.J.T., Kertész, Zs, Molnár, M., 2021. Source identification of PM_{2.5} carbonaceous aerosol using combined carbon fraction, radiocarbon and stable carbon isotope analyses in Debrecen, Hungary. *Sci. Total Environ.*, 146520 <https://doi.org/10.1016/j.scitotenv.2021.146520>.
- Marmureanu, L., Vasilescu, J., Slowik, J., Prévôt, A.S.H., Marin, C.A., Antonescu, B., Vlachou, A., Nemuc, A., Dandoci, A., Szidat, S., 2020. Online chemical characterization and source identification of summer and winter aerosols in Măgurele, Romania. *Atmosphere* 11, 385. <https://doi.org/10.3390/atmos11040385>.
- Na, K., Sawant, A., Song, C., Cocker, D., 2004. Primary and secondary carbonaceous species in the atmosphere of Western Riverside County, California. *Atmos. Environ.* 38, 1345–1355. <https://doi.org/10.1016/j.atmosenv.2003.11.023>.
- Nagy, Sz, Szabó, J., 2019. Characterization of PM_{2.5}-bound polycyclic aromatic hydrocarbons in the ambient air of Győr, Hungary. *Polycycl. Aromat. Compd.* 39 (4), 332–345. <https://doi.org/10.1080/10406638.2017.1326950>.
- National Census, 2022. Central statistics office. Available at: <https://nepszamlalas2022.ksh.hu/en/>. (Accessed 25 November 2024).
- Pachon, J., Weber, R., Zhang, X., Mulholland, J., Russell, A., 2013. Revising the use of potassium (K) in the source apportionment of PM_{2.5}. *Atmos. Pollut. Res.* 4. <https://doi.org/10.5094/APR.2013.002>.
- Piazzalunga, A., Belis, C., Bernardoni, V., Cazzuli, O., Fermo, P., Valli, G., Vecchi, R., 2011. Estimates of wood burning contribution to PM by the macro-tracer method using tailored emission factors. *Atmos. Environ.* 45 (37), 6642–6649. <https://doi.org/10.1016/j.atmosenv.2011.09.008>.
- Pulong, C., Tijian, W., Mei, D., Kasoar, M., Yong, H., Min, X., Shu, L., Bingliang, Z., Mengmeng, L., Tunan, H., 2017. Characterization of major natural and anthropogenic source profiles for size-fractionated PM in Yangtze River Delta. *Sci. Total Environ.* 598, 135–145. <https://doi.org/10.1016/j.scitotenv.2017.04.106>.
- Putaud, J.-P., Raes, F., Van Dingenen, R., Baltensperger, J.P.U., Brüggemann, E., Facchini, M.C., Decesari, S., Fuzzi, S., Gehrig, R., Hansson, H.C., Hueglin, C., Laj, P., Lorbeer, G., Maenhaut, W., Mihalopoulos, N., Müller, K., Querol, X., Rodriguez, S., Schneider, J., Spindler, G., ten Brink, H., Tørseth, K., Wehner, B., Wiedensohler, A., 2004. A European aerosol phenomenology. 2: chemical characteristics of particulate matter at kerbside, urban, rural and background sites in Europe. *Atmos. Environ.* 38, 2579–2595. <https://doi.org/10.1016/j.atmosenv.2004.01.041>.
- Putaud, J.-P., Van Dingenen, R., Alastuey, A., Bauer, H., Birmili, W., Cyrys, J., Flentje, H., Fuzzi, S., Gehrig, R., Hansson, H.C., Harrison, R.M., Herrmann, H., Hitenberger, R., Hüglin, C., Jones, A.M., Kasper-Giebl, A., Kiss, G., Kousa, A., Kuhlbusch, T.A.J., Loschnau, G., Maenhaut, W., Molnar, A., Moreno, T., Pekkanen, J., Perrino, C., Pitz, M., Puxbaum, H., Querol, X., Rodriguez, S., Salma, I., Schwarz, J., Smolik, J., Schneider, J., Spindler, G., ten Brink, H., Tursic, J., Viana, M., Wiedensohler, A., Raes, F., 2010. A European aerosol phenomenology – 3: physical and chemical characteristics of particulate matter from 60 rural, urban, and kerbside sites across Europe. *Atmos. Environ.* 44, 1308–1320. <https://doi.org/10.1016/j.atmosenv.2009.12.011>.
- Puxbaum, H., Caseiro, A., Sanchez-Ochoa, A., Kasper-Giebl, A., Claeys, M., Gelencsér, A., Legrand, M., Preunkert, S., Pio, C.A., 2007. Levoglucosan levels at background sites in Europe for assessing the impact of biomass combustion on the European aerosol background. *J. Geophys. Res.* 112, D23S04. <https://doi.org/10.1029/2006JD008114>.
- Ravindra, K., Sokhi, R., Van Grieken, R., 2008. Atmospheric polycyclic aromatic hydrocarbons: source attribution, emission factors and regulation. *Atmos. Environ.* 42, 2895–2921. <https://doi.org/10.1016/j.atmosenv.2007.12.010>.
- Reimer, P.J., Brown, T.A., Reimer, R.W., 2004. Discussion: reporting and calibration of post-bomb ¹⁴C Data. *Radiocarbon* 46, 1299–1304. <https://doi.org/10.1017/S0033822200033154>.
- Ricciardelli, I., Bacco, D., Rinaldi, M., et al., 2017. A three-year investigation of daily PM_{2.5} main chemical components in four sites: the routine measurement program of the Supersito Project (Po Valley, Italy). *Atmos. Environ.* 152, 418–430. <https://doi.org/10.1016/j.atmosenv.2016.12.052>.
- Roubicek, V., Raclavská, H., Juchelkova, D., Filip, P., 2008. Wear and environmental aspects of composite materials for automotive braking industry. *Wear* 265, 167–175. <https://doi.org/10.1016/j.wear.2007.09.014>.
- Sacco, P., Calisti, R., Mei, R., Boaretto, C., Quaglio, F., Zarin, L., 2019. Cyclopentanone: an unexpected airborne pollutant in a plastics moulding plant. *J. Occup. Environ. Hyg.* 10 (2), 53–105. <https://doi.org/10.36125/joehy.v10i2.319>.
- Salma, I., Némethy, Z., Weidinger, T., Maenhaut, W., Claeys, M., Molnár, M., Major, I., Ajtai, T., Utry, N., Bozóki, Z., 2017. Source apportionment of carbonaceous chemical species to fossil fuel combustion, biomass burning and biogenic emissions by a coupled radiocarbon–levoglucosan marker method. *Atmos. Chem. Phys.* 17, 13767–13781. <https://doi.org/10.5194/acp-17-13767-2017>.
- Salma, I., Vasanits-Zsigrai, A., Machon, A., Varga, T., Major, I., Gergely, V., Molnár, M., 2020. Fossil fuel combustion, biomass burning and biogenic sources of fine carbonaceous aerosol in the Carpathian Basin. *Atmos. Chem. Phys.* 20, 4295–4312. <https://doi.org/10.5194/acp-20-4295-2020>.
- Schmidl, C., Marr, I.L., Caseiro, A., Kotianová, P., Berner, A., Bauer, H., Kasper-Giebl, A., Puxbaum, H., 2008. Chemical characterisation of fine particle emissions from wood stove combustion of common woods growing in mid-European Alpine regions. *Atmos. Environ.* 42, 126–141. <https://doi.org/10.1016/j.atmosenv.2007.09.028>.
- Schwarz, J., Cusack, M., Karban, J., Chalupníková, E., Havránek, V., Smolik, J., Ždímal, V., 2016. PM_{2.5} chemical composition at a rural background site in Central Europe, including correlation and air mass back trajectory analysis. *Atmos. Res.* 176–177. <https://doi.org/10.1016/j.atmosres.2016.02.017>.
- Silibello, C., Calori, G., Costa, M.G., Mircea, M., Radice, P., Vitali, L., Zanini, G., 2012. Benzo(a)pyrene modelling over Italy: Comparison with experimental data and source apportionment. *Atmos. Pollut. Res.* 3, 399–407. <https://doi.org/10.5194/acp-21-17855-2021>.
- Sillanpää, M., Hillamo, R., Saarikoski, S., Frey, A., Pennanen, A., Makkonen, U., 2006. Chemical composition and mass closure of particulate matter at six urban sites in Europe. *Atmos. Environ.* 40 (2), S212–S223. <https://doi.org/10.1016/j.atmosenv.2006.01.063>.
- Simoneit, B.R.T., 2002. Biomass Burning—A review of organic tracers for smoke from incomplete combustion. *Appl. Geochem.* 17, 129–162. [https://doi.org/10.1016/S0883-2927\(01\)00061-0](https://doi.org/10.1016/S0883-2927(01)00061-0).
- Simoneit, B.R.T., 2015. Triphenylbenzene in urban atmospheres: a new PAH source tracer. *Polycycl. Aromat. Compd.* 35 (1), 3–15. <https://doi.org/10.1080/10406638.2014.883417>.
- Simoneit, B.R.T., Medeiros, P.M., Didyk, B.M., 2005. Combustion products of plastics as indicators for refuse burning in the atmosphere. *Environ. Sci. Technol.* 39, 6961–6970. <https://doi.org/10.1021/es050767x>.
- Századvég Foundation, 2018. Survey on domestic heating and opinion on air pollution of the Hungarian population conducted by the Századvég Foundation on behalf of the Ministry of Agriculture, 2018.

- Szidat, S., Ruff, M., Perron, N., Wacker, L., Synal, H.-A., Hallquist, M., Shannigrahi, A.S., Yttri, K.E., Dye, C., Simpson, D., 2009. Fossil and non-fossil sources of organic carbon (OC) and elemental carbon (EC) in Göteborg, Sweden. *Atmos. Chem. Phys.* 9, 1521–1535. <https://doi.org/10.5194/acp-9-1521-2009>.
- Szigeti, T., Óvári, M., Dunster, C., Kelly, F.J., Lucarelli, F., Zárny, Gy, 2015. Changes in chemical composition and oxidative potential of urban PM_{2.5} between 2010 and 2013 in Hungary. *Sci. Total Environ.* 518–519. <https://doi.org/10.1016/j.scitotenv.2015.03.025>.
- Tomšej, T., Horák, J., Tomšejová, S., Krpec, K., Klanová, J., Dej, M., Hopan, F., 2018. The impact of co-combustion of polyethylene plastics and wood in a small residential boiler on emissions of gaseous pollutants, particulate matter, PAHs and 1,3,5-triphenylbenzene. *Chemosphere* 196, 18–24. <https://doi.org/10.1016/j.chemosphere.2017.12.12>.
- Turpin, B.J., Lim, H.J., 2001. Species contribution to PM_{2.5} mass concentrations: revisiting common assumptions for estimating organic mass. *Aerosol Sci. Technol.* 35 (1), 602–610. <https://doi.org/10.1080/02786820119445>.
- Viana, M., Chi, X., Maenhaut, W., Cafmeyer, J., Querol, X., Alastuey, A., Mikuska, P., Večeřa, Z., 2006. Influence of sampling artefacts on measured PM, OC, and EC levels in carbonaceous aerosols in an urban area. *Aerosol Sci. Technol.* 40 (2), 107–117. <https://doi.org/10.1080/02786820500484388>.
- Wang, R., Balkanski, Y., Boucher, O., Bopp, L., Chappell, A., Ciais, P., Hauglustaine, D., Peñuelas, J., Tao, S., 2015. Sources, transport and deposition of iron in the global atmosphere. *Atmos. Chem. Phys.* 15, 6247–6270. <https://doi.org/10.5194/acp-15-6247-2015>.
- WHO IEA, IRENA, UNSD, World Bank, 2022. Tracking SDG 7: the Energy Progress Report. World Bank, Washington DC. © World Bank. License: Creative Commons Attribution—NonCommercial 3.0 IGO (CC BY-NC 3.0 IGO). <https://trackingsdg7.esmap.org/downloads>.
- World Health Organization, 2021. Household Air Pollution and Health. World Health Organization, Geneva. Available at: <https://www.who.int/news-room/fact-sheets/detail/household-air-pollution-and-health>.
- Yttri, K.E., Schnelle-Kreis, J., Maenhaut, W., Abbaszade, G., Alves, C., Bjerke, A., Bonnier, N., Bossi, R., Claeys, M., Dye, C., Evtuygina, M., García-Gacio, D., Hillamo, R., Hoffer, A., Hyder, M., Iinuma, Y., Jaffrezou, J.L., Kasper-Giebl, A., Kiss, G., López-Mahía, P.L., Pio, C., Piot, C., Ramirez-Santa-Cruz, C., Sciare, J., Teinilä, K., Vermeylen, R., Vicente, A., Zimmermann, R., 2005. An intercomparison study of analytical methods used for quantification of levoglucosan in ambient aerosol filter samples. *Atmos. Meas. Tech.* 8, 125–147. <https://doi.org/10.5194/amt-8-1>.
- Yunker, M.B., et al., 2002. PAHs in the Fraser River basin: a critical appraisal of PAH ratios as indicators of PAH source and composition. *Org. Geochem.* 33, 489–515. [https://doi.org/10.1016/S0146-6380\(02\)00002-5](https://doi.org/10.1016/S0146-6380(02)00002-5).
- Zárate, I., Ezcurra, A., Lacaux, J., Dinh, P., 2000. Emission factor estimates of cereal waste burning in Spain. *Atmos. Environ.* 34, 3183–3193. [https://doi.org/10.1016/S1352-2310\(99\)00254-X](https://doi.org/10.1016/S1352-2310(99)00254-X).
- Zdráhal, Z., Oliveira, J., Vermeylen, R., Claeys, M., Maenhaut, W., 2002. Improved method for quantifying levoglucosan and related monosaccharide anhydrides in atmospheric aerosols and application to samples from urban and tropical locations. *Environ. Sci. Technol.* 36, 747–753. <https://doi.org/10.1021/es015619v>.